

# A note on the eigenvalues, singular values, and eigenvectors of Toeplitz and Hankel matrices

Sven-Erik Ekström\*

Division of Scientific Computing, Department of Information Technology, Uppsala University

Stefano Serra-Capizzano†

Department of Science and High Technology, Insubria University - Como

INdAM Research Unit at Department of Science and High Technology, Insubria University - Como

Division of Scientific Computing, Department of Information Technology, Uppsala University

Paris Vassalos‡

Department of Informatics, Athens University of Economics and Business

March 15, 2022

## Abstract

In a series of recent papers the spectral behavior of the matrix sequence  $\{Y_n T_n(f)\}$  is studied in the sense of the spectral distribution, where  $Y_n$  is the main antidiagonal (or flip matrix) and  $T_n(f)$  is the Toeplitz matrix generated by the function  $f$ , with  $f$  being Lebesgue integrable and with real Fourier coefficients. This kind of study is also motivated by computational purposes for the solution of the related large linear systems using the (preconditioned) MINRES algorithm. Here we complement the spectral study with more results holding both asymptotically and for a fixed dimension  $n$ , and with regard to eigenvalues and singular values: the final target is the design of ad hoc procedures for the computation of the related spectra via matrix-less algorithms, with a cost being linear in the number of computed eigenvalues. We emphasize that the challenge of the case of non-monotone generating functions is considered in this note, for which the previous matrix-less algorithms fail. Numerical experiments are reported and commented, with the aim of showing in a visual way the theoretical analysis.

## 1 Introduction

In a number of recent papers [11, 16, 17] the spectral behavior of the matrix-sequence  $\{Y_n T_n(f)\}$  is studied in the sense of the spectral distribution, where

$$Y_n = \begin{bmatrix} & & & 1 \\ & & 1 & \\ & \ddots & & \\ 1 & & & \\ & 1 & & \\ & & \ddots & \\ & & & 1 \end{bmatrix}$$

is the main antidiagonal or flip matrix and  $T_n(f)$  is the Toeplitz matrix generated by the symbol  $f$ , with  $f$  being Lebesgue integrable and with real Fourier coefficients. Of course the singular values of  $T_n(f)$  and  $Y_n T_n(f)$  coincide, given the unitary character of the permutation matrix  $Y_n$ . This study has been complemented by the same type of analysis in the a multilevel context, where additional technical issues have been addressed [12, 18, 19], taking into account the specific difficulties of the multilevel setting.

In this note we focus our attention on studying the eigenvalues and eigenvectors of the resulting Hankel matrices, both asymptotically and for a fixed dimension  $n$ . In particular we study the spectral relationship between the Toeplitz matrix  $T_n(f)$  and the matrix  $Y_n T_n(f)$  and we furnish a more precise description of eigenvalues and eigenvectors of  $Y_n T_n(f)$  than in the previous literature, using also quite old results on the eigenstructure of Toeplitz matrices [5, 6].

\*sven-erik.ekstrom@it.uu.se

†s.serracapizzano@uninsubria.it

‡pvassal@aueb.gr

The practical target relies in designing ad hoc procedures for the computation of the related spectra via matrix-less algorithms (see [8] and references therein), with a cost being linear in the number of computed eigenvalues. Here the novelty relies in considering non-monotone generating functions, for which the previous matrix-less procedures usually fail; see [8, 10, 7] and references therein. Furthermore, this type of study is also motivated by other computational purposes such as the solution of the related large linear systems, using the (preconditioned) MINRES algorithm.

A careful selection of numerical tests is considered and the numerical experiments confirm the precise forecasts contained in the theoretical derivations.

The current work is organized as follows. In Section 2 we introduce the basic notions and we set the notation. Section 3 contains the theoretical analysis, while the numerical experiments are distributed in all the rest of the paper. Finally Section 4 is concerned with conclusions and open problems.

## 2 Notation and Basic Notions

The present section is divided into three parts. In Subsection 2.1 we report the definition of Toeplitz matrices and of the notion of generating function; Subsection 2.2 contains the analogous setting for Hankel matrices; finally Subsection 2.3 is devoted to the notions of eigenvalue and singular value distribution and to report and prove basic facts that will be used in the theoretical analysis.

### 2.1 Toeplitz Matrices and Matrix-Sequences

Let  $f \in L^1(-\pi, \pi)$  and let  $T_n(f)$  be the Toeplitz matrix generated by  $f$ , i.e.,  $(T_n(f))_{s,t} = \hat{f}_{s-t}$ ,  $s, t = 1, \dots, n$ , with  $f$  being the generating function of  $\{T_n(f)\}$  and with  $\hat{f}_k$  being the  $k$ -th Fourier coefficient of  $f$ , that is,

$$\hat{f}_k = \frac{1}{2\pi} \int_{-\pi}^{\pi} f(\theta) e^{-ik\theta} d\theta, \quad i^2 = -1, \quad k \in \mathbb{Z}. \quad (1)$$

If  $f$  is real-valued then several spectral properties are known (localization, extremal behavior, collective distribution, see [4, 20] and references therein) and  $f$  is also the spectral symbol of  $\{T_n(f)\}$  in the Weyl sense [4, 15, 24, 28]. If  $f$  is complex-valued, then the same type of information is transferred to the singular values, while the eigenvalues can have a 'wild' behavior [22] in some cases and a quite regular behavior in other cases [25]. More advanced material on distribution results are collected in the books on Generalized Locally Toeplitz matrix sequences [13, 14].

### 2.2 Hankel Matrices and Matrix-Sequences

The standard definition [4, Section 1.4] of Hankel matrices generated from a symbol  $f$  are the two matrices,

$$H_n^{(1)}(f) = [\hat{f}_{i+j-1}]_{i,j=1}^n, \quad H_n^{(2)}(f) = [\hat{f}_{-(i+j-1)}]_{i,j=1}^n,$$

or

$$H_n^{(1)}(f) = \begin{bmatrix} \hat{f}_1 & \hat{f}_2 & \hat{f}_3 & \cdots \\ \hat{f}_2 & \hat{f}_3 & \ddots & \ddots \\ \hat{f}_3 & \ddots & \ddots & \ddots \\ \vdots & \ddots & \ddots & \ddots \end{bmatrix}, \quad H_n^{(2)}(f) = \begin{bmatrix} \hat{f}_{-1} & \hat{f}_{-2} & \hat{f}_{-3} & \cdots \\ \hat{f}_{-2} & \hat{f}_{-3} & \ddots & \ddots \\ \hat{f}_{-3} & \ddots & \ddots & \ddots \\ \vdots & \ddots & \ddots & \ddots \end{bmatrix}.$$

Here we treat a different setting and we define the Hankel matrix  $H_n(f)$ , generated by the function  $f$ , as

$$H_n(f) = Y_n T_n(f) = H_n(1) T_n(f),$$

where  $T_n(f)$  is the Toeplitz matrix generated by  $f$  and

$$Y_n = H_n(1) = \begin{bmatrix} & & & 1 \\ & & 1 & \\ & \ddots & \ddots & \\ 1 & & & \end{bmatrix},$$

is the antidiagonal or "flip matrix", of size  $n$ . The matrix  $Y_n$  is a permutation matrix and hence it is unitary so that the singular values of  $T_n(f)$  and  $Y_n T_n(f)$  coincide, while for the eigenvalues there is a substantial (and computationally beneficial) change; see [16, 11, 12, 19, 18] and references therein.

### 2.3 Spectral and Singular Value Distributions

We now consider previous results concerning spectral distributions in the sense of Weyl. First we introduce some notations and definitions concerning general sequences of matrices. For any function  $F$  defined on the complex field and for any matrix  $A_n$  of size  $d_n$ , by the symbol  $\Sigma_\lambda(F, A_n)$ , we denote the mean

$$\Sigma_\lambda(F, A_n) = \frac{1}{d_n} \sum_{j=1}^{d_n} F[\lambda_j(A_n)],$$

while by the symbol  $\Sigma_\sigma(F, A_n)$ , we denote the mean

$$\Sigma_\sigma(F, A_n) = \frac{1}{d_n} \sum_{j=1}^{d_n} F[\sigma_j(A_n)].$$

**Definition 1** *Given a sequence  $\{A_n\}$  of matrices of size  $d_n$  with  $d_n < d_{n+1}$  and given a Lebesgue-measurable function  $\psi$  defined over a measurable set  $K \subset \mathbb{R}^\nu$ ,  $\nu \in \mathbb{N}^+$ , of finite and positive Lebesgue measure  $\mu(K)$ , we say that  $\{A_n\}$  is distributed as  $(\psi, K)$  in the sense of the eigenvalues if for any continuous  $F$  with bounded support the following limit relation holds*

$$\lim_{n \rightarrow \infty} \Sigma_\lambda(F, A_n) = \frac{1}{\mu(K)} \int_K F(\psi) d\mu. \quad (2)$$

*In this case, we write in short  $\{A_n\} \sim_\lambda (\psi, K)$ . Furthermore we say that  $\{A_n\}$  is distributed as  $(\psi, K)$  in the sense of the singular values if for any continuous  $F$  with bounded support the following limit relation holds*

$$\lim_{n \rightarrow \infty} \Sigma_\sigma(F, A_n) = \frac{1}{\mu(K)} \int_K F(|\psi|) d\mu. \quad (3)$$

*In this case, we write in short  $\{A_n\} \sim_\sigma (\psi, K)$ , which is equivalent to  $\{A_n^* A_n\} \sim_\lambda (|\psi|^2, K)$ .*

In Remark 1 we provide an informal meaning of the notion of eigenvalue distribution. For the singular value distribution similar statements can be written.

**Remark 1** *The informal meaning behind the above definition is the following. If  $\psi$  is continuous,  $n$  is large enough, and*

$$\left\{ \mathbf{x}_j^{(d_n)}, j = 1, \dots, d_n \right\}$$

*is an equispaced grid on  $K$ , then a suitable ordering  $\lambda_j(A_n)$ ,  $j = 1, \dots, d_n$ , of the eigenvalues of  $A_n$  is such that the pairs  $\left\{ \left( \mathbf{x}_j^{(d_n)}, \lambda_j(A_n) \right), j = 1, \dots, d_n \right\}$  reconstruct approximately the hypersurface*

$$\{(\mathbf{x}, \psi(\mathbf{x})), \mathbf{x} \in K\}.$$

*In other words, the spectrum of  $A_n$  ‘behaves’ like a uniform sampling of  $\psi$  over  $K$ , up to few outliers. For instance, if  $\nu = 1$ ,  $d_n = n$ , and  $K = [a, b]$ , then the eigenvalues of  $A_n$  are approximately equal to  $\psi(a + j(b - a)/n)$ ,  $j = 1, \dots, n$ , for  $n$  large enough and up to at most  $o(n)$  outliers. Analogously, if  $\nu = 2$ ,  $d_n = n^2$ , and  $K = [a_1, b_1] \times [a_2, b_2]$ , then the eigenvalues of  $A_n$  are approximately equal to  $\psi(a_1 + j(b_1 - a_1)/n, a_2 + k(b_2 - a_2)/n)$ ,  $j, k = 1, \dots, n$ , for  $n$  large enough and up to at most  $o(n^2)$  outliers. In general, when the symbol  $\psi$  is smooth enough, the number of outliers reduce and can decrease to  $O(1)$ : for instance, for Hermitian Toeplitz matrix sequences having generating function real-valued a.e. and with the range being a unique interval, the number of outliers is simply zero.*

The asymptotic distribution of eigen and singular values of a sequence of Toeplitz matrices has been thoroughly studied in the last century (for example see [4, 27] and the references reported therein). The starting point of this theory, which contains many extensions and other results, is a famous theorem of Szegő [15], which we report in the Tyrtynikov and Zamarashkin version [27].

**Theorem 1** *If  $f$  is integrable over  $Q$ , and if  $\{T_n(f)\}$  is the sequence of Toeplitz matrices generated by  $f$ , then*

$$\{T_n(f)\} \sim_\sigma (f, Q). \quad (4)$$

*Moreover, if  $f$  is also real-valued almost everywhere (a.e.), then each matrix  $T_n(f)$  is Hermitian and*

$$\{T_n(f)\} \sim_\lambda (f, Q). \quad (5)$$

On the other hand, if  $f$  is real-valued a.e., then very precise localization results are known. In fact, in that case all the eigenvalues of  $T_n(f)$  belong to the open interval  $(m, M)$ , where  $m$  and  $M$  are the essential infimum and the essential supremum of  $f$ , respectively, under the assumption that  $f$  is not constant a.e. In the general case where  $f$  is constant a.e., the result is trivial since  $T_n(f) \equiv mI_n$  for every matrix order  $n$ , with  $I_n$  being the identity matrix of size  $n$  (see [20, 3]). In any case, with regard to Remark 1, in this setting we do not observe the presence of outliers.

First we introduce the notion of equal distribution regarding (at least) two sequences of numerical sets of increasing cardinality. Then we state a selection of results which emphasize the relationships among equal distribution, uniform gridding, and spectral distribution of matrix-sequences (see also [23]). Part of the related material is taken from [21] and will be used in our subsequent derivations.

**Definition 2** Two sequences  $\{X_n\}$  and  $\{Y_n\}$  of numerical sets with  $X_n = \{x_j^{(d_n)}, j = 1, \dots, d_n\}$  and  $Y_n = \{y_j^{(d_n)}, j = 1, \dots, d_n\}$  are equally distributed if for any continuous  $F$  with bounded support the following limit relation holds

$$\lim_{n \rightarrow \infty} \frac{1}{d_n} \sum_{j=1}^{d_n} F(x_j^{(d_n)}) - F(y_j^{(d_n)}) = 0. \quad (6)$$

In the case where the two sequences of sets  $\{X_n\}$  and  $\{Y_n\}$  are made up by the spectra of two sequences of matrices  $\{A_n\}$  and  $\{B_n\}$  we write that the two sequences of matrices are spectrally equally distributed, while the two sequences are equally distributed in the singular value sense if (6) holds true and the two sequences of sets  $\{X_n\}$  and  $\{Y_n\}$  are made up by the sets of singular values of two sequences of matrices  $\{A_n\}$  and  $\{B_n\}$ .

**Remark 2** Of course, by playing with the given definitions, in the case where two sequences of matrices  $\{A_n\}$  and  $\{B_n\}$  are spectrally equally distributed, we have  $\{A_n\} \sim_{\lambda} (\psi, K)$  if and only if  $\{B_n\} \sim_{\lambda} (\psi, K)$ . Furthermore, in the case where two sequences of matrices  $\{A_n\}$  and  $\{B_n\}$  are equally distributed in the singular value sense, we have  $\{A_n\} \sim_{\sigma} (\psi, K)$  if and only if  $\{B_n\} \sim_{\sigma} (\psi, K)$ .

**Definition 3** A grid of points  $\{X_n\}$ ,  $X_n = \{x_j^{(d_n)}, j = 1, \dots, d_n\}$ , is uniformly distributed in  $[a, b]$  if and only if  $\{X_n\}$  and  $\{U_n\}$  are equally distributed with  $U_n = \{u_j^{(d_n)} = a + (b - a)j/d_n, j = 1, \dots, d_n\}$ .

More in general, a grid of points  $\{X_n\}$ ,  $X_n = \{\mathbf{x}_j^{(d_n)}, j = 1, \dots, d_n\}$ , is uniformly distributed in a Peano-Jordan measurable set  $K$ , contained in  $\mathbf{R}^d$  and of positive measure, if and only if for any  $d$  dimensional rectangle  $R$  contained in  $K$

$$\lim_{n \rightarrow \infty} \frac{1}{d_n} \sum_{j=1}^{d_n} \text{card} \{ \mathbf{x}_j^{(d_n)} \in R \} = \frac{\mu(R)}{\mu(K)}. \quad (7)$$

With the help of the previous concepts we can refine the statements contained in Remark 1 when the symbol  $\psi$  is continuous and  $K = [a, b]$ .

**Proposition 1** Assume  $\{A_n\} \sim_{\lambda} (\psi, K)$  with  $K = [a, b]$ ,  $\psi$  continuous, with the spectrum of  $A_n$  contained in  $\psi([a, b])$  for every  $n$ . Then there exists  $\{X_n\}$ ,  $X_n = \{x_j^{(d_n)}, j = 1, \dots, d_n\}$  uniformly distributed and contained in  $[a, b]$  such that

$$\lambda_j(A_n) = \psi(x_j^{(d_n)}).$$

Analogously, assume  $\{A_n\} \sim_{\sigma} (\psi, K)$  with  $K = [a, b]$ ,  $\psi$  continuous, with the spectrum of  $A_n$  contained in  $|\psi|([a, b])$  for every  $n$ . Then there exists  $\{X_n\}$ ,  $X_n = \{x_j^{(d_n)}, j = 1, \dots, d_n\}$  uniformly distributed and contained in  $[a, b]$  such that

$$\sigma_j(A_n) = |\psi(x_j^{(d_n)})|.$$

**Proof 1** Since the spectrum of  $A_n$  is contained in  $\psi([a, b])$ , it is clear that there exists  $\{X_n\}$ ,

$$X_n = \{x_j^{(d_n)}, j = 1, \dots, d_n\}$$

such that

$$\lambda_j(A_n) = \psi(x_j^{(d_n)}),$$

with  $x_j^{(d_n)} \in [a, b]$ ,  $\forall j = 1, \dots, d_n$ ,  $\forall n$ .

Now because of the assumption  $\{A_n\} \sim_{\lambda} (\psi, K)$  with  $K = [a, b]$ , for every continuous  $F$  (the boundedness of the image of the continuous function  $\psi$  allows to drop the assumption of bounded support), we find

$$\Sigma_{\lambda}(F, A_n) - \frac{1}{\mu(K)} \int_K F(\psi) d\mu = o(1),$$

as  $n \rightarrow \infty$ , which is the same as

$$\frac{1}{d_n} \sum_{j=1}^{d_n} F[\psi(x_j^{(d_n)})] - \frac{1}{\mu(K)} \int_K F(\psi) d\mu = o(1),$$

as  $n \rightarrow \infty$ . Given the arbitrary choice of  $F$  in the large class of continuous functions, in view of Definition 3, it follows that the grid sequence  $\{X_n\}$  is necessarily uniformly distributed in  $[a, b]$ .

The proof of the analogous claim for the singular values can be repeated verbatim as before.

The previous result can be easily generalized as stated in the subsequent two propositions, whose proofs follow substantially the same steps as in the proof of Proposition 1.

**Proposition 2** Assume  $\{A_n\} \sim_{\lambda} (\psi, K)$  with  $K$  Peano-Jordan measurable and of positive measure,  $\psi$  continuous, with the spectrum of  $A_n$  contained in  $\psi(K)$  for every  $n$ . Then there exists  $\{X_n\}$ ,  $X_n = \{x_j^{(d_n)}, j = 1, \dots, d_n\}$  uniformly distributed and contained in  $K$  such that

$$\lambda_j(A_n) = \psi(x_j^{(d_n)}).$$

Analogously, assume  $\{A_n\} \sim_{\sigma} (\psi, K)$  with  $K$  Peano-Jordan measurable and of positive measure,  $\psi$  continuous, with the spectrum of  $A_n$  contained in  $|\psi|(K)$  for every  $n$ . Then there exists  $\{X_n\}$ ,  $X_n = \{x_j^{(d_n)}, j = 1, \dots, d_n\}$  uniformly distributed and contained in  $K$  such that

$$\sigma_j(A_n) = |\psi(x_j^{(d_n)})|.$$

**Proposition 3** Assume  $\{A_n\} \sim_{\lambda} (\psi, K)$  with  $K$  Peano-Jordan measurable and of positive measure,  $\psi$  Riemann integrable. Then there exists  $\{X_n\}$ ,  $X_n = \{x_j^{(d_n)}, j = 1, \dots, d_n\}$  uniformly distributed and contained in  $K$  such that

$$\{\{\lambda_j(A_n) : j = 1, \dots, d_n\}\}, \quad \left\{ \left\{ \psi(x_j^{(d_n)}) \mid j = 1, \dots, d_n \right\} \right\}$$

are equally distributed. Analogously, assume  $\{A_n\} \sim_{\sigma} (\psi, K)$  with  $K$  Peano-Jordan measurable and of positive measure,  $\psi$  Riemann integrable. Then there exists  $\{X_n\}$ ,  $X_n = \{x_j^{(d_n)}, j = 1, \dots, d_n\}$  uniformly distributed and contained in  $K$  such that

$$\{\{\lambda_j(A_n) : j = 1, \dots, d_n\}\}, \quad \left\{ \left\{ |\psi(x_j^{(d_n)})| \mid j = 1, \dots, d_n \right\} \right\}$$

are equally distributed.

### 3 Eigenstructure of Flipped Toeplitz matrices

By combining old and recent results we describe specific properties related to the eigenstructure of flipped Toeplitz matrices. We start with a simple lemma regarding the matrix  $H_n(1)$ . Then the rest of the section is divided into three subsections. Subsection 3.1 treats eigenvalues and eigenvectors of  $H_n(f)$  in the case where  $f$  is even and real-valued (which corresponds to real Fourier coefficients with  $\hat{f}_k = \hat{f}_{-k}$  any integer  $k$ ); Subsection 3.2 treats eigenvalues and eigenvectors of  $H_n(f)$  in the case where  $f$  is complex-valued and the Fourier coefficients are real.

**Lemma 1** One eigendecomposition of the antidiagonal  $H_n(1)$  is described as follow

$$H_n(1) = \mathbb{S}_n \mathbb{H}_n \mathbb{S}_n,$$

where  $\mathbb{H}_n$  is a diagonal matrix

$$\mathbb{H}_n = \begin{bmatrix} 1 & & & & & \\ & -1 & & & & \\ & & 1 & & & \\ & & & -1 & & \\ & & & & \ddots & \\ & & & & & (-1)^{n+1} \end{bmatrix},$$

that is,  $(\mathbb{H}_n)_{i,i} = (-1)^{i+1}$  and  $\mathbb{S}_n$  is the unitary discrete sine transform

$$\begin{aligned}\mathbb{S}_n &= \sqrt{\frac{2}{n+1}} \left( \sin \left( \frac{ij\pi}{n+1} \right) \right)_{i,j=1}^n \\ &= [\mathbf{v}_1^{(n)}, \mathbf{v}_2^{(n)}, \dots, \mathbf{v}_n^{(n)}],\end{aligned}\tag{8}$$

where  $\mathbf{v}_j^{(n)}$  is the  $j$ th column,

$$\mathbf{v}_j^{(n)} = \sqrt{\frac{2}{n+1}} \begin{bmatrix} \sin(j\pi/(n+1)) \\ \sin(2j\pi/(n+1)) \\ \vdots \\ \sin(nj\pi/(n+1)) \end{bmatrix}.\tag{9}$$

## Proof 2

$$\begin{aligned}H_n(1)\mathbb{S}_n &= \sqrt{\frac{2}{n+1}} \left( \sin \left( \frac{(n+1-i)j\pi}{n+1} \right) \right)_{i,j=1}^n \\ &= \sqrt{\frac{2}{n+1}} \left( \sin \left( j\pi - \frac{ij\pi}{n+1} \right) \right)_{i,j=1}^n \\ &= \sqrt{\frac{2}{n+1}} \left( \sin(j\pi) \cos \left( \frac{ij\pi}{n+1} \right) - \cos(j\pi) \sin \left( \frac{ij\pi}{n+1} \right) \right)_{i,j=1}^n \\ &= \sqrt{\frac{2}{n+1}} \left( (-1)^{j+1} \sin \left( \frac{ij\pi}{n+1} \right) \right)_{i,j=1}^n \\ &= [\mathbf{v}_1^{(n)}, -\mathbf{v}_2^{(n)}, \mathbf{v}_3^{(n)}, -\mathbf{v}_4^{(n)}, \dots, (-1)^{n+1}\mathbf{v}_n^{(n)}]\end{aligned}$$

Since  $\mathbb{S}_n$  is unitary, it follows that  $\mathbb{S}_n H(1)\mathbb{S}_n = \mathbb{H}_n$ .

### 3.1 Real Symmetric Case

#### 3.1.1 Eigenvalues

**Theorem 2** For a symbol  $f$  that generates a real symmetric Toeplitz matrix  $T_n(f)$  for every  $n$ , we infer that the eigenvalues of  $H_n(f) = H_n(1)T_n(f)$  and  $T_n(f)$  are related as follows

$$\lambda_j(H_n(f)) = (-1)^{j+1} \lambda_j(T_n(f)),\tag{10}$$

where  $\lambda_j(T_n(f))$  are ordered as the samplings of the symbol  $f(\xi_{\Pi_n(j),n})$ , with  $\lambda_j(T_n(f)) = f(\xi_{\Pi_n(j),n})$ ,  $\Pi_n$  proper permutation, and

$$0 \leq \xi_{1,n} \leq \xi_{2,n} \leq \dots \leq \xi_{n,n} \leq \pi,\tag{11}$$

with  $\{\{\xi_{j,n} : j = 1, \dots, n\}\}$  equally distributed in  $[0, \pi]$ .

**Proof 3** Assume a matrix  $X_n$  and  $X_n \mathbf{v} = \lambda \mathbf{v}$ , that is,  $\mathbf{v}$  is an eigenvector of  $X_n$  and  $\lambda$  is the corresponding eigenvalue.

If we have one of the following two cases,

a.  $H_n(1)\mathbf{v} = \mathbf{v}$ ,

b.  $H_n(1)\mathbf{v} = -\mathbf{v}$ ,

then respectively

$$H_n(1)X_n \mathbf{v} = H_n(1)\lambda \mathbf{v} = \lambda \mathbf{v},$$

$$H_n(1)X_n \mathbf{v} = H_n(1)\lambda \mathbf{v} = -\lambda \mathbf{v}.$$

We notice that any matrix  $X_n$  belonging to the  $\tau$  class [1, 2, 9] is diagonalized by the sine transform  $\mathbb{S}_n$  reported in (8), whose columns  $\mathbf{v}_j^{(n)}$ ,  $j = 1, \dots, n$ , given (9) enjoy alternatively either a. or b., as shown in the proof

of Lemma 1. Since the  $\tau$  class includes any tridiagonal Toeplitz matrix generated by a function  $f$  of the form  $f(\theta) = a + 2b \cos(\theta)$ ,  $a, b \in \mathbf{R}$ , with

$$T_n(f) = \begin{bmatrix} a & b & \cdots & 0 & 0 & & & \\ b & a & \ddots & \ddots & \ddots & \ddots & & \\ \vdots & \ddots & \ddots & \ddots & \ddots & \ddots & 0 & \\ 0 & \ddots & \ddots & \ddots & \ddots & \ddots & 0 & \\ 0 & \ddots & \ddots & \ddots & \ddots & \ddots & \vdots & \\ & \ddots & \ddots & \ddots & \ddots & a & b & \\ & & 0 & 0 & \dots & b & a & \end{bmatrix},$$

it follows that relation (10) holds with

$$\lambda_j(T_n(f)) = f\left(\frac{j\pi}{n+1}\right), \quad j = 1, \dots, n,$$

so that the grid

$$\left\{ \xi_{\Pi_n(j),n} = \frac{j\pi}{n+1} \right\}$$

is perfectly known and  $\Pi_n = I$  for any  $n$  with  $I$  identity matrix.

When the bandwidth is larger than 3, but fixed with respect to  $n$ , the continuous function  $f$  is such that  $f(\theta) = f(-\theta)$  (since the Fourier coefficients are real) and hence it can be uniformly approximated in infinity norm by a sequence of trigonometric cosine polynomials. Furthermore, in such a setting, either property a. or property b. holds as proven in [5, 6] and hence the desired relation (10) is satisfied. To conclude, the fact that  $\lambda_j(T_n(f)) = f(\xi_{\Pi_n(j),n})$ ,  $\Pi_n$  proper permutation, and  $\{\{\xi_{j,n} : j = 1, \dots, n\}\}$  as in (11) equally distributed in  $[0, \pi]$  and belonging to  $(0, \pi)$  is now a consequence of Theorem 1, taking into account the continuity of the generating function  $f$  and the localization results [20, 3], as discussed just after Theorem 1.

It should be remarked that the result just proven can be easily extended to the case of piece-wise continuous symbols and in the widest generalization to the case where  $f$  is just Riemann integrable. The hint of the proof relies on the fact that the sequence of sets obtained by evaluating the function  $f$  on a equally distributed grid is distributed as  $f$ .

Now the main question concerns how to characterize the sequence of permutations  $\Pi_n$ . Interestingly enough the proof of Theorem 2 informs that  $\Pi_n = I$  when  $f$  is a linear cosine polynomial this is the general case in the terms reported in the statement below for the eigenvalues of  $T_n(f)$ .

**Theorem 3** *With reference to the assumptions of Theorem 2, the sequence of permutations  $\Pi_n$  can be chosen as the sequence of identity matrices.*

**Remark 3** *In the case of a non-monotone  $f$  in Theorem 3, the best ordering of the eigenvalues and hence the “perfect grid”  $\xi_{j,n}$  in (11) is not obvious if we want to rely on an asymptotic expansion as in the monotone setting. Hence, in these cases the eigenvalues of  $H_n(f)$  might give insights regarding the correct ordering of the eigenvalues of  $T_n(f)$ . A substantial benefit is that a matrix-less method could then be employed also for some non-monotone symbols (see [8] and references there reported).*

Take, for example, the symbol  $f(\theta) = \cos(\theta) + \cos(2\theta)$ . In the left panel of Figure 1 we see the symbol  $f(\theta)$  (green line), equispaced samplings of the symbol  $f(\theta_{j,n})$  (green circles), and the eigenvalues of  $T_n(f)$  (yellow circles), for  $n = 10$ . The eigenvalues are ordered with a permutation  $\Pi_n^{-1}(j)$ , such that,  $f(\theta_{\Pi_n(1),n}) \leq \dots \leq f(\theta_{\Pi_n(n),n})$  (since  $f$  is non-monotone different grid samplings might coincide, in that case we order the samplings  $f(\theta_{\Pi_n(j),n})$  according to the index  $j$ ). The “perfect grid”  $\xi_{j,n}$ , such that  $f(\xi_{j,n}) = \lambda_j(T_n(f))$ , is computed numerically for the ordering given the permutation  $\Pi_n^{-1}(j)$ . However, since the symbol  $f$  is non-monotone, we expect that the ordering  $\Pi_n(j)^{-1}$  might be not the most precise (we define it on a grid  $\theta_{j,n}$  instead of the true unknown, and non-unique,  $\xi_{j,n}$ ). Hence, the approximated  $\xi_{j,n}$  might be not optimal.

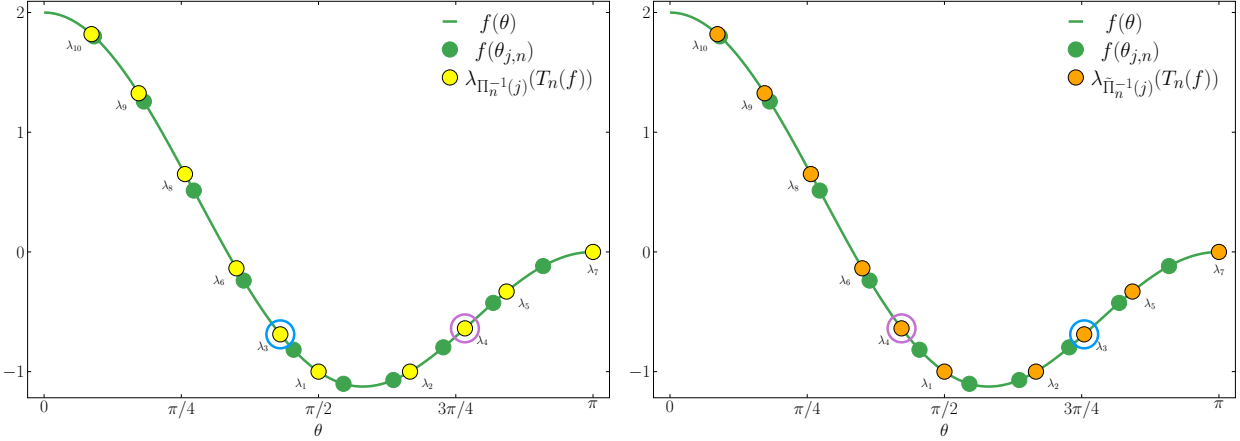


Figure 1: [Ordering of eigenvalues (non-monotone symmetric symbol,  $f(\theta) = \cos(\theta) + \cos(2\theta)$ )] Left: Ordering  $\Pi_n^{-1}(j)$  (match with symbol samplings  $f(\theta_{j,n})$ ) Right: Ordering  $\tilde{\Pi}_n^{-1}(j)$ , where two eigenvalues ( $\lambda_3$  and  $\lambda_4$ ) switch places, due to a mismatch with the signs of the eigenvalues of  $H_n(f)$ .

In Table 1 we first present the permutations  $\Pi_n(j)$  and  $\Pi_n^{-1}(j)$ , and the samplings of the symbol  $f(\theta)$  with the grid  $\theta_{j,n} = j\pi/(n+1)$  for  $j = 1, \dots, n$ , and  $n = 10$ .

Then, the eigenvalues  $\lambda_{\Pi_n^{-1}(j)}(T_n(f))$  are listed. For a correct ordering of the eigenvalues we assume, from Conjecture 3, that  $(-1)^{j+1}\lambda_{\Pi_n^{-1}(j)}(T_n(f))$  should coincide with  $\lambda_{\rho(j)}(H_n(f))$  (where  $\rho(j)$  is a permutation such that  $|\lambda_{\Pi_n^{-1}(j)}(T_n(f))| = |\lambda_{\rho(j)}(H_n(f))|$ ; of course in the rare case of multiplicity larger than one then the permutation is adapted). Highlighted in red, in the last two columns, we see a mismatch in signs for the fifth and eighth eigenvalues (of the permuted ordering  $\Pi_n^{-1}(j)$ , that is the original eigenvalues  $\lambda_3$  (blue) and  $\lambda_4$  (pink)). These two eigenvalues are highlighted in the left panel of Figure 1; blue and pink circle respectively.

Table 1: [Ordering of eigenvalues (non-monotone symmetric symbol,  $f(\theta) = \cos(\theta) + \cos(2\theta)$ )] Ordering of the eigenvalues using permutation  $\Pi_n^{-1}(j)$  gives a mismatch of two values (signs), highlighted in red, of  $(-1)^{j+1}\lambda_{\Pi_n^{-1}(j)}(T_n(f))$  and  $\lambda_{\rho(j)}(H_n(f))$ .

| $j$ | $\Pi_n(j)$ | $\Pi_n^{-1}(j)$ | $f(\theta_{j,n})$ | $\lambda_{\Pi_n^{-1}(j)}(T_n(f))$ | $(-1)^{j+1}\lambda_{\Pi_n^{-1}(j)}(T_n(f))$ | $\lambda_{\rho(j)}(H_n(f))$ |
|-----|------------|-----------------|-------------------|-----------------------------------|---|-----------------------------|
| 1   | 6          | 10              | 1.8007            | 1.8193                            | 1.8193                                      | 1.8193                      |
| 2   | 7          | 9               | 1.2567            | 1.3255                            | -1.3255                                     | -1.3255                     |
| 3   | 5          | 8               | 0.5125            | 0.6502                            | 0.6502                                      | 0.6502                      |
| 4   | 8          | 6               | -0.2394           | -0.1369                           | 0.1369                                      | 0.1369                      |
| 5   | 9          | 3               | -0.8172           | <b>-0.6886</b>                    | <b>-0.6886</b>                              | <b>0.6886</b>               |
| 6   | 4          | 1               | -1.1018           | -1.0000                           | 1.0000                                      | 1.0000                      |
| 7   | 10         | 2               | -1.0703           | -1.0000                           | -1.0000                                     | -1.0000                     |
| 8   | 3          | 4               | -0.7972           | <b>-0.6386</b>                    | <b>0.6386</b>                               | <b>-0.6386</b>              |
| 9   | 2          | 5               | -0.4258           | -0.3309                           | -0.3309                                     | -0.3309                     |
| 10  | 1          | 7               | -0.1182           | 0.0000                            | 0.0000                                      | 0.0000                      |

In Table 2 we show the alternative permutations  $\tilde{\Pi}_n(j)$  and  $\tilde{\Pi}_n^{-1}(j)$ ; defined such that  $\lambda_3$  and  $\lambda_4$  are switched in  $\tilde{\Pi}_n(j)$ . As seen, the values  $(-1)^{j+1}\lambda_{\tilde{\Pi}_n^{-1}(j)}(T_n(f))$  and  $\lambda_{\tilde{\rho}(j)}(H_n(f))$  (where  $\tilde{\rho}(j)$  is the equivalent ordering as  $\rho(j)$  but for  $\tilde{\Pi}_n^{-1}(j)$  instead of  $\Pi_n^{-1}(j)$ ) now match. In the right panel of Figure 1 we report the eigenvalues with the new ordering  $\tilde{\Pi}_n^{-1}(j)$ .

Table 2: [Ordering of eigenvalues (non-monotone symmetric symbol,  $f(\theta) = \cos(\theta) + \cos(2\theta)$ )] Ordering of the eigenvalues using permutation  $\tilde{\Pi}_n^{-1}(j)$ , where two eigenvalues have switched places, does not give a missmatch of  $(-1)^{j+1} \lambda_{\tilde{\Pi}_n^{-1}(j)}(T_n(f))$  and  $\lambda_{\tilde{\rho}(j)}(H_n(f))$  (as in Table 1).

| $j$ | $\tilde{\Pi}_n(j)$ | $\tilde{\Pi}_n^{-1}(j)$ | $f(\theta_{j,n})$ | $\lambda_{\tilde{\Pi}_n^{-1}(j)}(T_n(f))$ | $(-1)^{j+1} \lambda_{\tilde{\Pi}_n^{-1}(j)}(T_n(f))$ | $\lambda_{\tilde{\rho}(j)}(H_n(f))$ |
|-----|--------------------|-------------------------|-------------------|---|--|-------------------------------------|
| 1   | 6                  | 10                      | 1.8007            | 1.8193                                    | 1.8193   | 1.8193                              |
| 2   | 7                  | 9                       | 1.2567            | 1.3255                                    | -1.3255  | -1.3255                             |
| 3   | 8                  | 8                       | 0.5125            | 0.6502                                    | 0.6502   | 0.6502                              |
| 4   | 5                  | 6                       | -0.2394           | -0.1369                                   | 0.1369   | 0.1369                              |
| 5   | 9                  | 4                       | -0.8172           | -0.6386                                   | -0.6386  | -0.6386                             |
| 6   | 4                  | 1                       | -1.1018           | -1.0000                                   | 1.0000   | 1.0000                              |
| 7   | 10                 | 2                       | -1.0703           | -1.0000                                   | -1.0000  | -1.0000                             |
| 8   | 3                  | 3                       | -0.7972           | -0.6886                                   | 0.6886   | 0.6886                              |
| 9   | 2                  | 5                       | -0.4258           | -0.3309                                   | -0.3309  | -0.3309                             |
| 10  | 1                  | 7                       | -0.1182           | 0.0000                                    | 0.0000   | 0.0000                              |

### 3.1.2 Numerical verification 1 of Remark 3

A closely related matrix, to the Toeplitz matrix  $T_n(f)$  in Remark 3, is the Toeplitz-like matrix  $T_{n,0,0} = T_n(f) - R_n$  where  $R_n$  is a low-rank matrix with 1/2 in the top left and bottom right corners;  $T_{n,\varepsilon,\varphi}(f)$  is the generated matrix by the symbol  $f$  belonging to the  $\tau_{\varepsilon,\varphi}$ -algebra; e.g., see [1, 2, 9]. For all matrices  $T_{n,\varepsilon,\varphi}(f)$ , where  $\varepsilon, \varphi \in \{-1, 0, 1\}$  we know the full eigendecomposition and ‘‘perfect grids’’  $\xi_{j,n}$ ; e.g.,  $\lambda_j(T_{j,0,0}(f)) = f(\theta_{j,n})$  and  $\mathbb{Q}_n$  is the discrete sine transform, DST. Hence, the eigenvectors of  $T_n(f)$  are closely related to the DST (asymptotically they coincide), and we can assume that eigenvector  $\mathbf{v}_{\tilde{\Pi}_n^{-1}(j)}$  of  $T_n(f)$  should behave approximately as  $\sin(j\theta_{i,n})$ .

In Figure 2 we show the fifth (left panels) and eighth (right panels) DST (non-normalized) eigenvectors ( $\sin(5\theta)$  and  $\sin(8\theta)$ ).

In the top two panels of Figure 2 we show the fifth and eighth eigenvectors using the permutation  $\tilde{\Pi}_n^{-1}(j)$  (the original  $\lambda_3(T_n(f))$  and  $\lambda_4(T_n(f))$ ). A clear mismatch is present and perturbing the grid  $\theta_{j,n}$  will not yield a ‘‘perfect grid’’  $\xi_{j,n}$  to match the eigenvector elements with the DST. In the bottom two panels of Figure 2 we show the fifth and eighth eigenvectors using the permutation  $\tilde{\Pi}_n^{-1}(j)$  (the original  $\lambda_4(T_n(f))$  and  $\lambda_3(T_n(f))$ ). A much better match between the eigenvector elements and the DST is present.

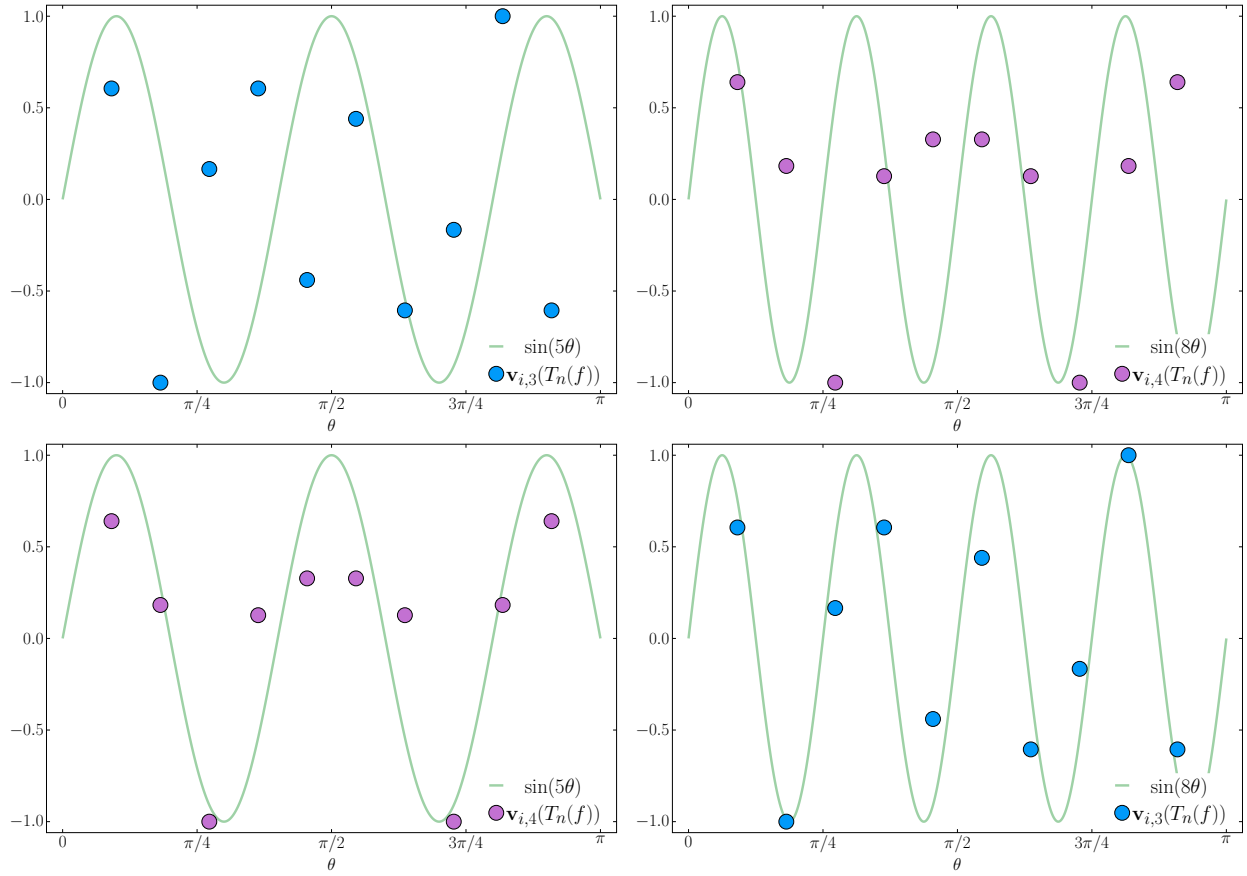


Figure 2: [Ordering of eigenvalues (non-monotone symmetric symbol,  $f(\theta) = \cos(\theta) + \cos(2\theta)$ )] Left panels: Eigenvector five, with permutation  $\Pi_n^{-1}(j)$  (top) and  $\tilde{\Pi}_n^{-1}(j)$  (bottom). Right panels: Same as left panels, but for eigenvector eight.

In Figure 3 we present a numerically computed (non-unique) grid  $\xi_{j,n}$  such that the eigenvector elements matches the DST. Again, note that the DST is simply an approximation of the eigenvectors of  $T_n(f)$ , but Figures 2 and 3 are good indications that the modified permutation  $\tilde{\Pi}_n^{-1}(j)$  is a better ordering of the eigenvalues, than  $\Pi_n^{-1}(j)$ .

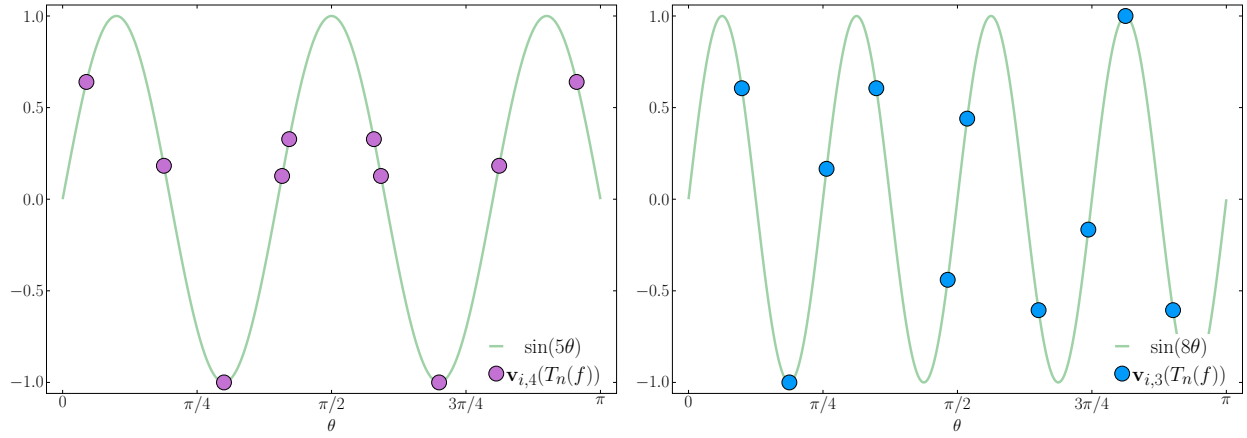


Figure 3: [Ordering of eigenvalues (non-monotone symmetric symbol,  $f(\theta) = \cos(\theta) + \cos(2\theta)$ )] Left panel: Eigenvector five,  $\tilde{\Pi}_n^{-1}(j)$  using a numerically computed ‘‘perfect grid’’. Right panel: Same as left panel, but for eigenvector eight.

### 3.1.3 Numerical verification 2 of Remark 3

In Section 3.1.2 we assumed that we knew that eigenvectors five and eight (after reordering according to the symbol) should be switched. If this type of ‘‘true ordering’’ of eigenvalues of Toeplitz matrices  $T_n(f)$ , generated by non-monotone symbols, is to be used in practical applications (e.g., matrix-less methods) we suggest a more

automatic approach. We here propose an outline of an algorithm to find the “true ordering” of the eigenvalues, for a given  $n$ . The algorithm can be summarized as follows: We are interested in the ordering of the eigenvalues of a matrix  $T_n(f)$ , generated by the symbol  $f(\theta)$ . Construct a matrix  $\hat{T}_n(f)$ , which has the same symbol  $f$ , where the full eigendecomposition is known. This can for example be the matrices generated by the  $\tau_{\varepsilon,\varphi}$ -algebras [1, 2, 9]. Now define  $R_n = T_n(f) - \hat{T}_n(f)$  and  $B_n^{(\gamma)} = \hat{T}_n(f) + \gamma R_n$ , and  $\gamma \in [0, 1]$ . We now assume that the elements of same index eigenvectors for matrices  $B_n^{(\gamma)}$  vary continuously as  $\gamma$  is varied from zero to one. Hence, we here study the matrix sequence  $\{B_n^{(\gamma)}\}_\gamma$ , for  $\gamma \in [0, 1]$ .

**Algorithm 1 (Automatic ordering  $\tilde{\Pi}_n^{-1}(j)$  of eigenvalues)**

1. Define:

- $T_n(f)$ : Matrix of interest (we note that this approach should work for more general Toeplitz-like matrices);
- $f(\theta)$ : Symbol of the matrix  $T_n(f)$  (here assumed to be univariate, scalar valued and real-symmetric for simplicity);
- $\hat{T}_n(f)$ : Matrix, with symbol  $f$ , for which full eigendecomposition is known (e.g.,  $T_{n,\varepsilon,\varphi}(f)$ ,  $\varepsilon, \varphi \in \{-1, 0, 1\}$ );
- $R_n = T_n(f) - \hat{T}_n(f)$ : Low-rank matrix such that  $B_n^{(\gamma)} = \hat{T}_n(f) + \gamma R_n$ ,  $\gamma \in [0, 1]$ .  $B_n^{(0)} = \hat{T}_n(f)$  and  $B_n^{(1)} = T_n(f)$ ;
- $N_{\text{steps}}$ : Number of matrices to generate in the algorithm, from  $\hat{T}_n(f)$  and  $T_n(f)$ ;
- $\gamma_k = (k-1)/(N_{\text{steps}} - 1)$ ,  $k = 1, \dots, N_{\text{steps}}$

2. We have,  $\lambda_j(B_n^{(0)}) = f(\xi_{j,n})$  and  $\mathbf{v}_j(B_n^{(0)})$  (e.g., if  $\hat{T}_n(f) = T_{n,0,0}(f)$ , we have  $\xi_{j,n} = j\pi/(n+1)$  and  $\mathbf{v}_j(B_n^{(0)}) = \sqrt{2/(n+1)} \sin(j\xi_{j,n})$ ).

3. Iterate  $k = 2, \dots, N_{\text{steps}}$

- (a) Numerically compute the eigenvalues and eigenvectors of  $B_n^{(\gamma_k)}$ , called  $\lambda_j(B_n^{(\gamma_k)})$  and  $\mathbf{v}_j(B_n^{(\gamma_k)})$ . Ordering is given by the numerical solver (often in non-decreasing order);
- (b) Iterate  $j = 1, \dots, n$ , and minimize  $\epsilon_j = \|\mathbf{v}_r(B_n^{(\gamma_{k-1})}) - \mathbf{v}_j(B_n^{(\gamma_k)})\|_2$  for  $r \in 1, \dots, n$ . Call each of these indices  $r_j$ . Take into account,
  - comparison with both  $\mathbf{v}_j(B_n^{(\gamma_k)})$  and  $-\mathbf{v}_j(B_n^{(\gamma_k)})$ ;
  - for less computational effort, only consider the eigenvectors  $\mathbf{v}_r(B_n^{(\gamma_{k-1})})$  with  $r$  corresponding to eigenvalues  $\lambda_r(B_n^{(\gamma_{k-1})})$  close to the eigenvalue  $\lambda_j(B_n^{(\gamma_k)})$ ;
  - two eigenvectors  $\mathbf{v}_j(B_n^{(\gamma_k)})$  may minimize the norm  $\epsilon_j$  to the same eigenvector  $\mathbf{v}_r(B_n^{(\gamma_{k-1})})$ ; This is the ordering  $\tilde{\rho}(j)$ .
- (c) Reorder the eigenvalues and eigenvectors for step  $k$  according to the ordering  $r_j$ ,  $j = 1, \dots, n$ ;

4. The final ordering  $(\tilde{\Pi}_n^{-1}(j))$  where  $\gamma = 1$ , should be the “true ordering” of  $T_n(f)$ .

For the example in Remark 3, we have  $n = 10$ ,  $f(\theta) = \cos(\theta) + \cos(2\theta)$ , and the choice of  $\hat{T}_n(f) = T_{n,0,0}(f)$ ,

$$T_n(f) = \frac{1}{2} \begin{bmatrix} 0 & 1 & 1 & & & & & & & \\ 1 & 0 & 1 & 1 & & & & & & \\ 1 & 1 & 0 & 1 & 1 & & & & & \\ & \ddots & \ddots & \ddots & \ddots & \ddots & & & & \\ & & 1 & 1 & 0 & 1 & 1 & & & \\ & & & 1 & 1 & 0 & 1 & & & \\ & & & & 1 & 1 & 0 & 1 & & \\ & & & & & 1 & 1 & 0 & 1 & \\ & & & & & & 1 & 1 & 0 & \\ & & & & & & & 1 & 1 & 0 \end{bmatrix}, \quad \hat{T}_n(f) = T_{n,0,0}(f) = \frac{1}{2} \begin{bmatrix} -1 & 1 & 1 & & & & & & & \\ 1 & 0 & 1 & 1 & & & & & & \\ 1 & 1 & 0 & 1 & 1 & & & & & \\ & \ddots & \ddots & \ddots & \ddots & \ddots & \ddots & & & \\ & & 1 & 1 & 0 & 1 & 1 & & & \\ & & & 1 & 1 & 0 & 1 & 1 & & \\ & & & & 1 & 1 & 0 & 1 & 1 & \\ & & & & & 1 & 1 & -1 & & \end{bmatrix},$$

and

$$R_n = T_n(f) - \hat{T}_n(f) = \frac{1}{2} \begin{bmatrix} 1 & & & & & & \\ & 0 & & & & & \\ & & \ddots & & & & \\ & & & 0 & & & \\ & & & & 1 & & \\ & & & & & 1 & \\ & & & & & & 1 \end{bmatrix},$$

and  $B_n^{(\gamma)} = T_{n,0,0}(f) + \gamma R_n$ .

In Figure 4 we show the ten eigenvalues, ordered as  $\Pi_n^{-1}(j)$  (left) and, automatically by Algorithm 1,  $\tilde{\Pi}_n^{-1}(j)$  (right), for the matrices  $B_n^{(\gamma)}$  as  $\gamma$  is varied from 0 to 1 over  $N_{steps} = 100$  steps. The dashed black line indicates a  $\gamma_b = (103 - 13\sqrt{41})/80 \approx 0.247$  where eigenvalues five and eight of  $\Pi_n^{-1}(j)$  switch places (visible as the eigenvalue curves cross, and  $\lambda_5(B_n^{(\gamma_b)}) = \lambda_8(B_n^{(\gamma_b)}) = (9 + \sqrt{41})/20 \approx 0.770$ ).

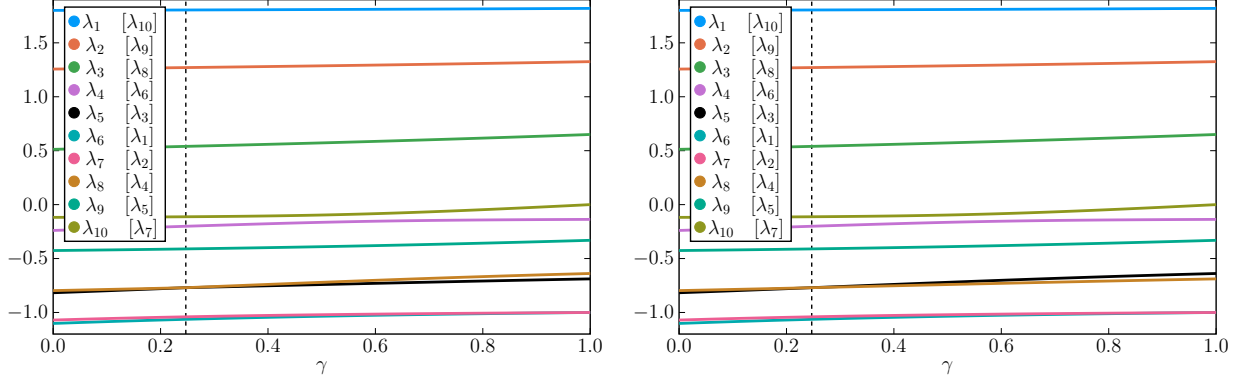


Figure 4: [Ordering of eigenvalues (non-monotone symmetric symbol,  $f(\theta) = \cos(\theta) + \cos(2\theta)$ )] Eigenvalues for  $B_{10}^{(\gamma_k)}$ ,  $k = 1, \dots, N_{steps}$  with ordering  $\Pi_n^{-1}(j)$  (left) and  $\tilde{\Pi}_n^{-1}(j)$  (right). In the left panel, the switch of  $\lambda_5$  and  $\lambda_8$  does not occur at  $\gamma_b$  (dashed black line), whereas it does so in the right panel.

In Figure 5 we show the eigenvector elements for eigenvector five (left) and eight (right) for the matrices  $B_n^{(\gamma)}$ . On top we sort the eigenvalues (and corresponding eigenvectors) solely comparing with the samplings  $f(\theta_{j,n})$ , i.e.  $\Pi_n^{-1}(j)$ . In the bottom we switch (automatically, using Algorithm 1) the eigenvectors five and eight for all  $\gamma \geq \gamma_b$ , and consequently we obtain the resulting ordering  $\tilde{\Pi}_n^{-1}(j)$ . Note that here  $\lambda_5$  and  $\lambda_8$  are the third and fourth eigenvalues in the original non-decreasing monotone ordering by the numerical solver.

Yellow circles denote the eigenvector elements for  $\gamma = 0$ , that is  $T_{n,0,0}(f)$ . Blue circles correspond to the eigenvector elements for intermediate matrices; as  $\gamma$  increases, so does the size of the circles. Red circles corresponds to the eigenvector elements of  $T_n(f)$ . All vectors in the figure are normalized (and with choice of sign to correspond to the signs of the vectors forming the DST matrix).

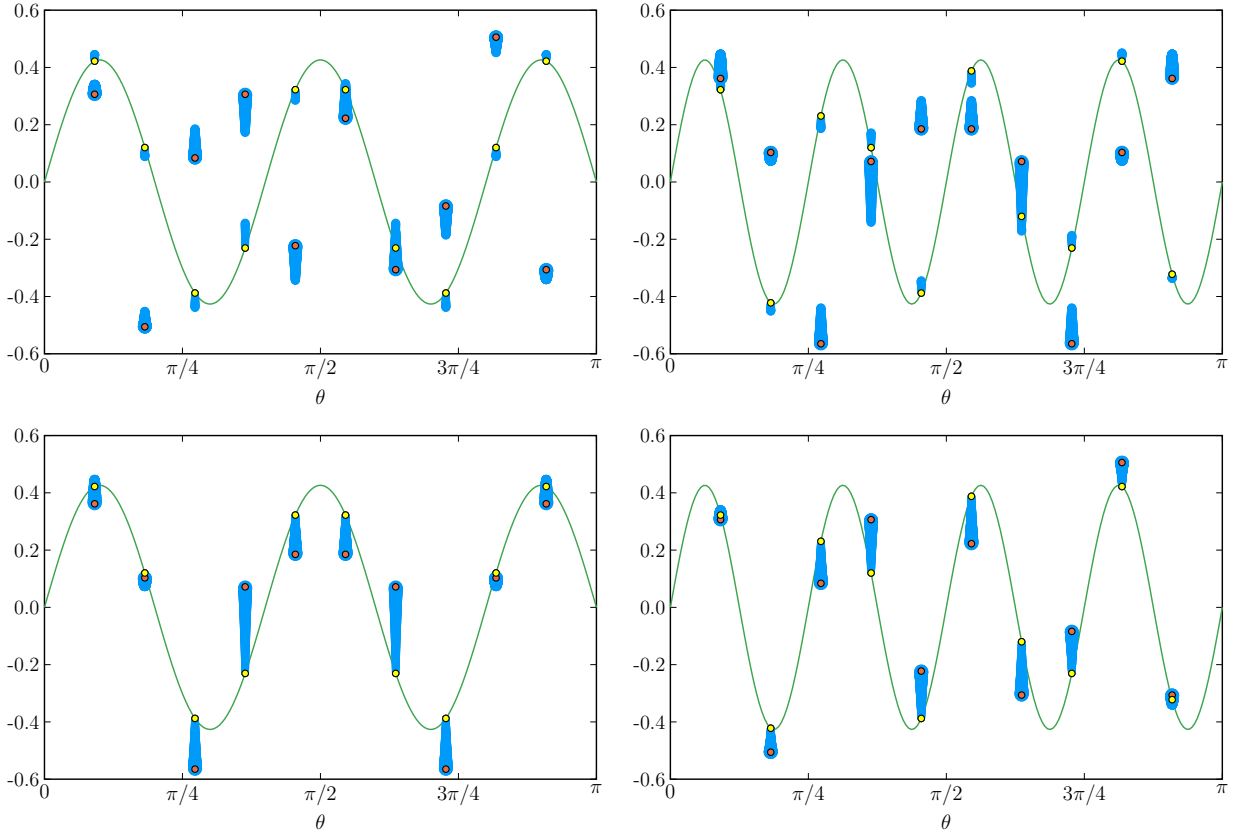


Figure 5: [Ordering of eigenvalues (non-monotone symmetric symbol,  $f(\theta) = \cos(\theta) + \cos(2\theta)$ )] Eigenvectors five (left) and eight (right) for  $B_{10}^{(\gamma_k)}$ ,  $k = 1, \dots, N_{steps}$  with ordering  $\Pi_n^{-1}(j)$  (top) and  $\tilde{\Pi}_n^{-1}(j)$  (bottom). Clear erratic behavior is visible in the top panels where the switch does not occur for the ordering of eigenvalues five and eight.

We here also note that the degenerate eigenvalues  $\lambda_6(T_n(f)) = \lambda_7(T_n(f)) = 1$ , of  $T_n(f)$  for  $n = 10$ , will typically yield “erratic” eigenvectors with respect to the sequence of eigenvector elements, as shown in Figure 6.

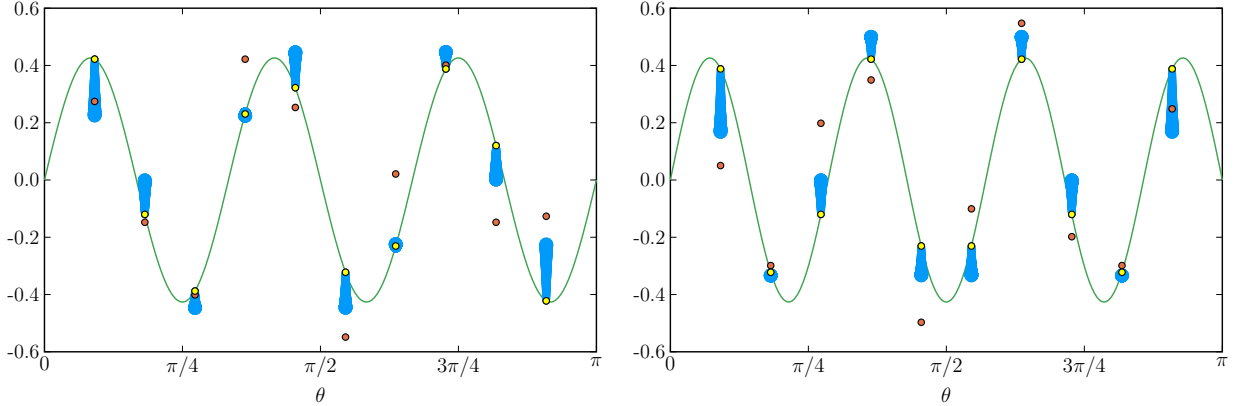


Figure 6: [Ordering of eigenvalues (non-monotone symmetric symbol,  $f(\theta) = \cos(\theta) + \cos(2\theta)$ )] Eigenvectors six and seven, for  $\gamma = 1$  (red circles), correspond to degenerative eigenvalues (equal to one), and the numerically computed eigenvectors behave “erratic” with respect to the sequence of elements.

Finally, we mention that as shown in Figure 6, also  $\hat{T}_n(f)$  (or any of the matrices  $B_n^{(\gamma_k)}$ ) can have degenerate eigenvalues. In Figure 7 we see that  $T_{n,0,0}(f)$  (left) has two eigenvalues that coincide, whereas  $T_{n,1,1}(f)$  (right) does not. However,  $T_{n,1,1}(f)$  does have two eigenvalues that switch order (four and nine), but that is handled automatically by Algorithm 1. Also, the presumed signs of the eigenvalues of  $H_n(f)$  match this computed ordering.

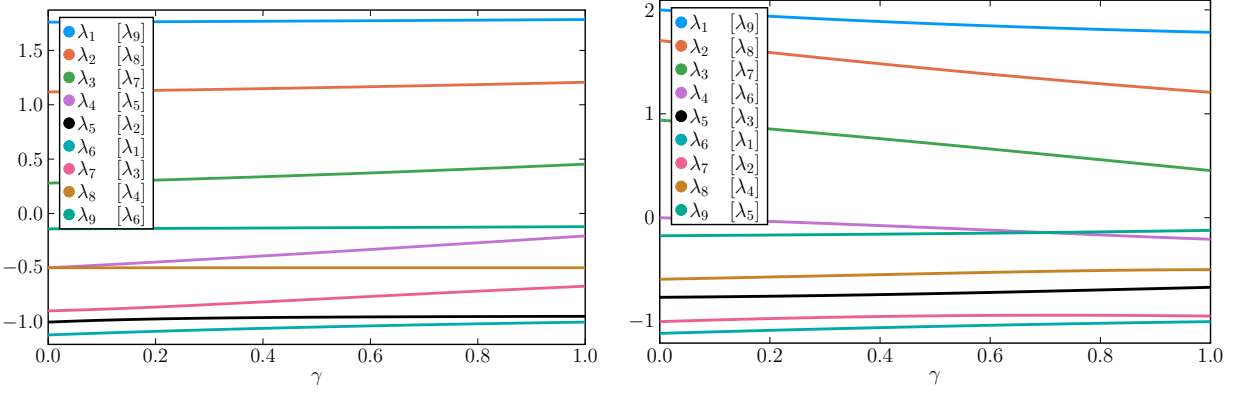


Figure 7: [Ordering of eigenvalues (non-monotone symmetric symbol,  $f(\theta) = \cos(\theta) + \cos(2\theta)$ )] Eigenvalues for  $B_n^{\gamma_k}$  with  $\hat{T}_n(f) = T_{n,0,0}(f)$  (left) and  $\hat{T}_n(f) = T_{n,1,1}(f)$  (right).

### 3.1.4 Eigenvectors

The eigenvectors of  $H_n(f)$  and  $T_n(f)$  are the same for a real-valued even generating function  $f$  (that is  $\hat{f}_k = \hat{f}_{-k}$  any integer  $k$ , all being real). In the case where  $f$  is complex-valued but the Fourier coefficients are real, the left-eigenvectors of  $T_n(f)$  coincide with the eigenvectors of the real symmetric matrix  $H_n(f)$ .

**Proof 4** Use same arguments as in Proof 3.

## 3.2 Real Non-Symmetric Case

### 3.2.1 Eigenvalues

**Conjecture 1** The eigenvalues of  $H_n(f)$  where  $f$  is non-symmetric real-valued is related to the singular values of  $T_n(f)$  as follows

$$\lambda_j(H_n(f)) = (-1)^{j+1} \sigma_j(T_n(f)),$$

where  $\sigma_j(T_n(f))$  are ordered as the samplings of the symbol  $f(\xi_{j,n})f(-\xi_{j,n})$ , where  $\sigma_j(T_n(f)) = \sqrt{f(\xi_{j,n})f(-\xi_{j,n})} = |f(\xi_{j,n})|$  and

$$0 \leq \xi_{1,n} \leq \xi_{2,n} \leq \dots \leq \xi_{n,n} \leq \pi. \quad (12)$$

### Numerical verification 1 of Conjecture 1

We study the two non-symmetric real matrices  $T_n(f_1)$  and  $T_n(f_2)$  generated by  $f_1(\theta) = 1 + e^{i\theta}$  and  $f_2(\theta) = 1 - e^{i\theta}$ ,

$$T_n(f_1) = \begin{bmatrix} 1 & & & & \\ 1 & 1 & & & \\ & \ddots & \ddots & & \\ & & & 1 & 1 \end{bmatrix}, \quad T_n(f_2) = \begin{bmatrix} 1 & & & & \\ -1 & 1 & & & \\ & \ddots & \ddots & & \\ & & & -1 & 1 \end{bmatrix}.$$

Since the entries of  $T_n(f)$  are real, we have  $\sigma_j(T_n(f)) = \sqrt{\lambda_j(T_n(f)^T T_n(f))}$ , where here the corresponding positive definite matrices are

$$T_n(f_1)^T T_n(f_1) = \begin{bmatrix} 2 & 1 & & & \\ 1 & 2 & 1 & & \\ & \ddots & \ddots & \ddots & \\ & & 1 & 2 & 1 \\ & & & 1 & 1 \end{bmatrix}, \quad T_n(f_2)^T T_n(f_2) = \begin{bmatrix} 2 & -1 & & & \\ -1 & 2 & -1 & & \\ & \ddots & \ddots & \ddots & \\ & & -1 & 2 & -1 \\ & & & -1 & 1 \end{bmatrix},$$

with associated symbols  $g_1(\theta) = |f_1(\theta)|^2 = f_1(-\theta)f_1(\theta) = 2 + 2\cos(\theta)$  and  $g_2(\theta) = |f_2(\theta)|^2 = f_2(-\theta)f_2(\theta) = 2 - 2\cos(\theta)$ . The matrix  $T_n(f_1)^T T_n(f_1)$  is the matrix  $T_{n,0,-1}(g_1)$ , belonging to the  $\tau_{0,-1}$ -algebra, where the eigenvalues are given exactly by  $g_1(\theta_{j,n}^{(0,-1)})$  where  $\theta_{j,n}^{(0,-1)} = j\pi/(n+1/2)$ . Hence,  $\sigma_{\Pi_n^{-1}(j)}(T_n(f_1)) = \sqrt{g_1(\theta_{j,n}^{(0,-1)})}$ .

Similarly, the singular values  $\sigma_{\Pi_n^{-1}(j)}(T_n(f_2)) = \sqrt{g_2(\theta_{j,n}^{(0,1)})}$ , since  $T_n(f_2)^T T_n(f_2)$  belongs to the  $\tau_{0,1}$ -algebra and  $\theta_{j,n}^{(0,1)} = (j-1/2)\pi/(n+1/2)$ .

Indeed,  $\lambda_{\rho(j)}(H_n(f_1))$  and  $(-1)^{j+1} \sqrt{g_1(\theta_{j,n}^{(0,-1)})}$  (and  $\lambda_{\rho(j)}(H_n(f_2))$  and  $(-1)^{j+1} \sqrt{g_2(\theta_{j,n}^{(0,1)})}$ ) match. Furthermore, we note that  $\lambda_{\rho(j)}(H_n(f_1)) = -\lambda_{\rho(j)}(H_n(f_2))$ .

**Proof 5** We first study the symbol  $f_1(\theta) = 1 + e^{i\theta}$ , where

$$H_n(f_1) = \begin{bmatrix} & & 1 & 1 \\ & \ddots & \ddots & \ddots \\ 1 & 1 & \ddots & \ddots \\ 1 & & & \ddots \end{bmatrix} \quad (13)$$

By a permutation matrix  $P$ , we have

$$P^{-1}H_n(f_1)P = \begin{bmatrix} 1 & 1 & & \\ 1 & 0 & 1 & \\ & \ddots & \ddots & \ddots \\ & & 1 & 0 & 1 \\ & & & 1 & 0 \end{bmatrix}. \quad (14)$$

This permuted matrix is the generated matrix  $T_{n,1,0}(2\cos(\theta))$ , by the  $\tau_{1,0}$ -algebra, and the eigenvalues are given exactly by,

$$\lambda_j(P^{-1}H_n(f_1)P) = 2\cos(\theta_{j,n}^{1,0}), \quad \theta_{j,n}^{1,0} = \frac{(j-1/2)\pi}{n+1/2}. \quad (15)$$

Note that the ordering, with this sampling grid, of these eigenvalues does not correspond to the ordering of the eigenvalues  $\lambda_j(H_n(f_1))$ , assuming Conjecture 1 is correct and the true ordering is given by

$$\lambda_j(H_n(f_1)) = (-1)^{j+1} \sqrt{2 + 2\cos\left(\frac{j\pi}{n+1/2}\right)} = (-1)^{j+1} 2\cos\left(\frac{j\pi}{2n+1}\right), \quad j = 1, \dots, n. \quad (16)$$

Hence, we show that the set of samplings of (16) and

$$2\cos\left(\frac{(j-1/2)\pi}{n+1/2}\right) = 2\cos\left(\frac{(2j-1)\pi}{2n+1}\right), \quad j = 1, \dots, n, \quad (17)$$

coincide (not the same order).

We note that for all odd  $j$ , the quantity in (16) is exactly

$$2\cos\left(\frac{j\pi}{2n+1}\right), \quad (18)$$

which is equivalent to  $j = 1, \dots, \lceil n/2 \rceil$  of (17).

For even  $j$ , the quantity in (16) is the same as

$$-2\cos\left(\frac{j\pi}{2n+1}\right), \quad (19)$$

which is equivalent to  $j = n, n-1, \dots, \lceil n/2 \rceil + 1$  of (17).

Now we study the symbol  $f_2(\theta) = 1 - e^{i\theta}$ , where

$$H_n(f_2) = \begin{bmatrix} & & -1 & 1 \\ & \ddots & \ddots & \ddots \\ -1 & 1 & & \\ 1 & & & \ddots \end{bmatrix}, \quad (20)$$

and by a permutation matrix  $P$ ,

$$P_1^{-1}H_n(f_2)P_1 = \begin{bmatrix} \begin{bmatrix} -1 & 1 \\ 1 & 0 \end{bmatrix} & \begin{bmatrix} 0 & 0 \\ -1 & 0 \end{bmatrix} & \begin{bmatrix} 0 & 0 \\ 0 & 1 \end{bmatrix} & \begin{bmatrix} 0 & 0 \\ 1 & 0 \end{bmatrix} \\ \begin{bmatrix} 0 & -1 \\ 0 & 0 \end{bmatrix} & \begin{bmatrix} 0 & 0 \\ 1 & 0 \end{bmatrix} & \begin{bmatrix} 0 & 0 \\ -1 & 0 \end{bmatrix} & \begin{bmatrix} 0 & 0 \\ 1 & 0 \end{bmatrix} \\ \ddots & \ddots & \ddots & \ddots \end{bmatrix}. \quad (21)$$

The matrix-valued symbol of this matrix is

$$f_p(\theta) = \begin{bmatrix} 0 & 1 - e^{i\theta} \\ 1 - e^{-i\theta} & 0 \end{bmatrix}, \quad (22)$$

which can be split into the two eigenvalue functions

$$f_p^{(1)} = \sqrt{2 - 2 \cos(\theta)} = 2 \sin(\theta/2) \quad (23)$$

$$f_p^{(2)} = -\sqrt{2 - 2 \cos(\theta)} = -2 \sin(\theta/2) \quad (24)$$

By direct inspection we find

$$\lambda_j(P^{-1}H_n(f_1)P) = \begin{cases} f_p^{(1)}(\theta_{\hat{j}, \lceil n/2 \rceil}^{(1)}), & j \text{ odd}, \\ f_p^{(2)}(\theta_{\hat{j}, \lfloor n/2 \rfloor}^{(2)}), & j \text{ even}, \end{cases} \quad \hat{j} = \lceil j/2 \rceil, \quad (25)$$

$$\theta_{\hat{j}, \lceil n/2 \rceil}^{(1)} = \frac{(2\hat{j} - 3/2)\pi}{n + 1/2}, \quad \hat{j} = 1, \dots, \lceil n/2 \rceil, \quad (26)$$

$$\theta_{\hat{j}, \lfloor n/2 \rfloor}^{(2)} = \frac{(2\hat{j} - 1/2)\pi}{n + 1/2}, \quad \hat{j} = 1, \dots, \lfloor n/2 \rfloor, \quad (27)$$

which is equivalent to

$$= (-1)^{j+1} \sqrt{2 - 2 \cos\left(\frac{(j - 1/2)\pi}{n + 1/2}\right)} = (-1)^{j+1} 2 \sin\left(\frac{(j - 1/2)\pi}{2n + 1}\right). \quad (28)$$

### Numerical verification 2 of Conjecture 1

The generating symbol for the Grcar matrix [26] is  $f(\theta) = -e^{i\theta} + 1 + e^{-i\theta} + e^{-2i\theta} + e^{-3i\theta}$ . Since we are interested in the singular values  $\sigma_j(T_n(f))$  we will now work with the modulus of the symbol  $|f(\theta)|$  (left panel in Figure 8), or more precisely taking the square root of the eigenvalues of the normal matrix  $(T_n(f))^T T_n(f)$  which has the symbol  $g(\theta) = f(-\theta)f(\theta) = 5 + 4 \cos(\theta) + 2 \cos(2\theta) - 2 \cos(4\theta)$  (right panel in Figure 8). The reason for this is that we can construct the matrix  $\hat{T}_n(g)$  needed in Algorithm 1.

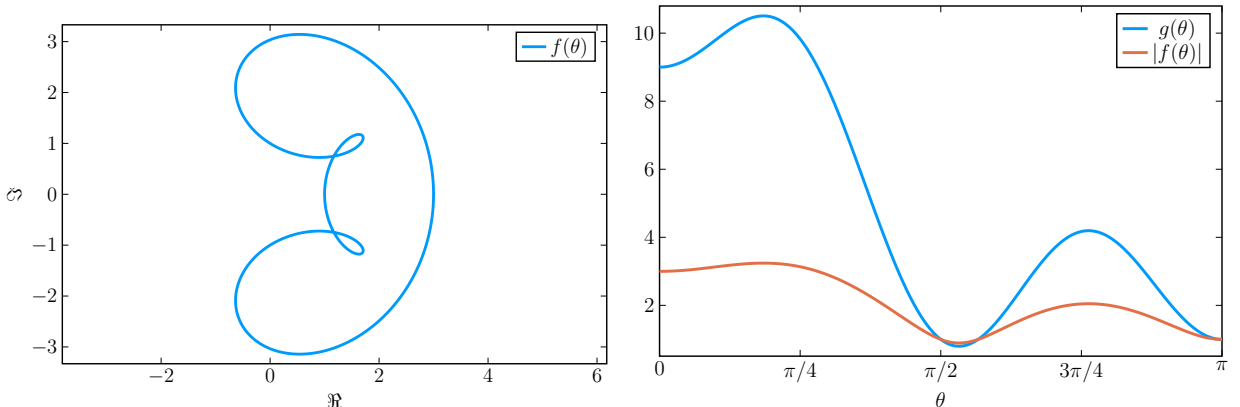


Figure 8: [Ordering of singular values (non-monotone non-symmetric symbol,  $f(\theta) = -e^{i\theta} + 1 + e^{-i\theta} + e^{-2i\theta} + e^{-3i\theta}$ )] Left: Complex valued symbol  $f(\theta)$ . Right:  $g(\theta) = f(-\theta)f(\theta)$  and  $|f(\theta)|$  on  $\theta \in [0, \pi]$ .

Below we show the matrices needed for Algorithm 1 where  $\hat{T}_n(g) = T_{n,0,0}(g)$  and the target matrix is

In Figure 9 we show the square root of the eigenvalues (such that, the sequence yield the singular values of the true target matrix  $T_n(f)$ ), for  $n = 10$ , for all  $B_n^{(\gamma_k)}$ , with  $N_{\text{steps}} = 100$ . The numbering in the figure is after the permutation  $\tilde{\Pi}_n^{-1}(j)$ . The yellow boxes indicate where it is visible that Algorithm 1 fails to swap singular values  $\sigma_5$  and  $\sigma_{10}$ , two times. However, since the swap fails twice the resulting ordering is correct. The blue circle indicates an erroneous ordering, when comparing with the signs of  $\lambda_j(H_n(f))$ , as indicated in Table 3

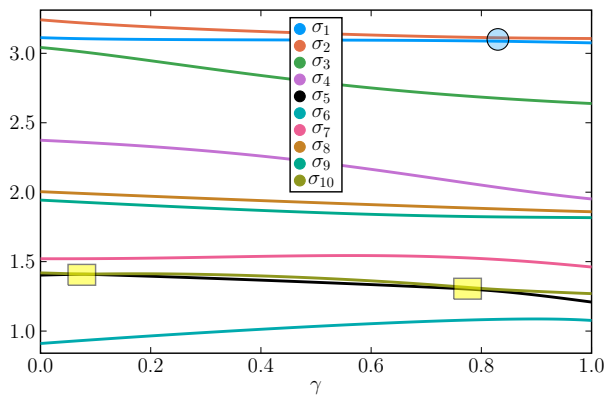


Figure 9: [Ordering of singular values (non-monotone non-symmetric symbol,  $f(\theta) = -e^{i\theta} + 1 + e^{-i\theta} + e^{-2i\theta} + e^{-3i\theta}$ )]  $\hat{T}_n(f) = T_{n,0,0}(f)$ .

In Table 3 we see that indeed  $\sigma_5$  and  $\sigma_{10}$  can be assumed to be correctly ordered. However,  $\sigma_1$  and  $\sigma_2$  are wrongly ordered, if Conjecture 1 is correct. Increasing  $N_{\text{steps}}$  to a higher number does not seem to remedy this discrepancy.

Table 3: [Ordering of eigenvalues (non-monotone non-symmetric symbol,  $f(\theta) = -e^{i\theta} + 1 + e^{-i\theta} + e^{-2i\theta} + e^{-3i\theta}$ )  
 $\hat{T}_n(f) = T_{n,0,0}(f)$ .

| $j$ | $\tilde{\Pi}_n(j)$ | $\tilde{\Pi}_n^{-1}(j)$ | $ f(\theta_{j,n}) $ | $\sigma_{\tilde{\Pi}_n^{-1}(j)}(T_n(f))$ | $(-1)^{j+1}\sigma_{\tilde{\Pi}_n^{-1}(j)}(T_n(f))$ | $\lambda_{\tilde{\rho}(j)}(H_n(f))$ |
|-----|--------------------|-------------------------|---------------------|--|--|-------------------------------------|
| 1   | 6                  | 9                       | 3.1128              | 3.0752                                   | <b>3.0752</b>                                      | -3.0752                             |
| 2   | 5                  | 10                      | 3.2412              | 3.1066                                   | <b>-3.1066</b>                                     | 3.1066                              |
| 3   | 10                 | 8                       | 3.0420              | 2.6384                                   | 2.6384   | 2.6384                              |
| 4   | 7                  | 7                       | 2.3741              | 1.9512                                   | -1.9512  | -1.9512                             |
| 5   | 9                  | 2                       | 1.4028              | 1.2089                                   | 1.2089   | 1.2089                              |
| 6   | 8                  | 1                       | 0.9106              | 1.0765                                   | -1.0765  | -1.0765                             |
| 7   | 4                  | 4                       | 1.5209              | 1.4612                                   | 1.4612   | 1.4612                              |
| 8   | 3                  | 6                       | 2.0037              | 1.8592                                   | -1.8592  | -1.8592                             |
| 9   | 1                  | 5                       | 1.9431              | 1.8166                                   | 1.8166   | 1.8166                              |
| 10  | 2                  | 3                       | 1.4191              | 1.2696                                   | -1.2696  | -1.2696                             |

In Figure 10 we report the ten eigenvector element sequences shown, given by Algorithm 1. One can clearly see the erratic behavior in eigenvectors five and ten, as previously indicated in Figure 9. However, eigenvectors one and two are visually correct.

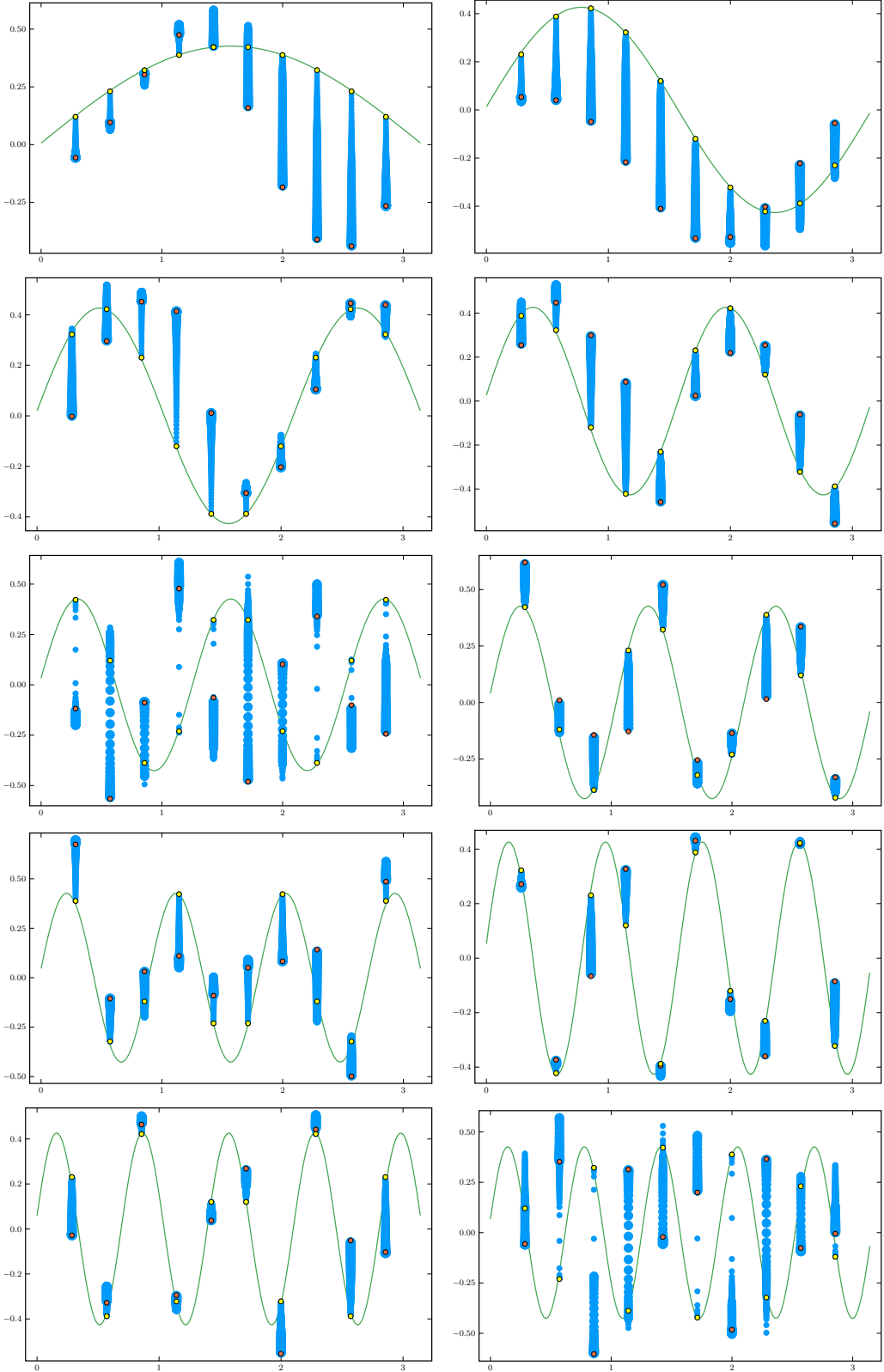


Figure 10: [Ordering of singular values (non-monotone non-symmetric symbol,  $f(\theta) = -e^{i\theta} + 1 + e^{-i\theta} + e^{-2i\theta} + e^{-3i\theta}$ )] All ten eigenvector sequences, except the fifth and tenth, seem to be continuous and correct.

In Figure 11 we show the sequences of  $B_n^{(\gamma_k)}$  for all combinations of  $\hat{T}_n(f) = T_{n,\varepsilon,\varphi}(f)$ ,  $\varepsilon, \varphi = \{-1, 0, -1\}$ . In Table 4 are shown the actual yielded orderings. As it can be seen, they all exhibit errors, and the different  $\hat{T}_n(f)$  have different bias to the initial ordering, and subsequent result. In Table 5 the corrected orderings are displayed and, given the used Algorithm 1, four acceptable versions are given.

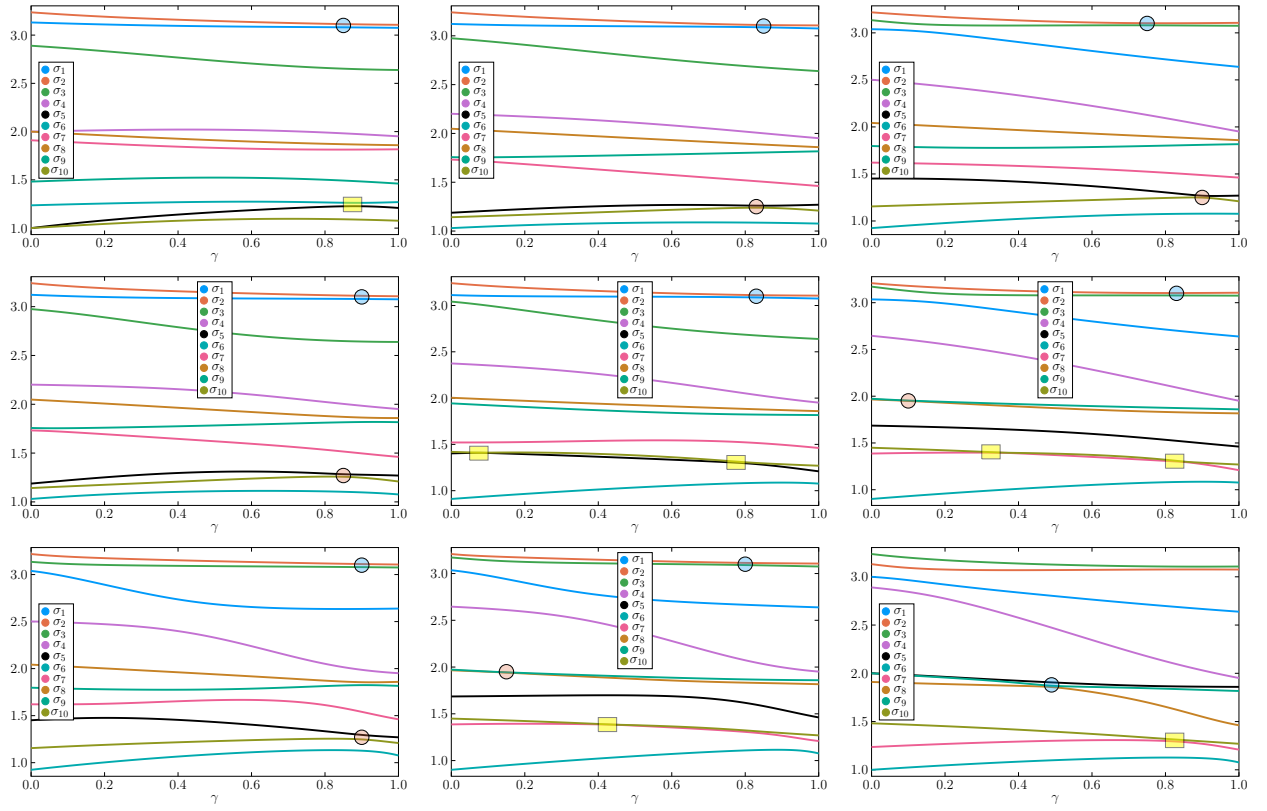


Figure 11: [Ordering of eigenvalues (non-monotone non-symmetric symbol,  $f(\theta) = -e^{i\theta} + 1 + e^{-i\theta} + e^{-2i\theta} + e^{-3i\theta}$ )  $\hat{T}_n(f) = T_{n,\varepsilon,\varphi}(f)$  for all combinations  $\varepsilon, \varphi = \{-1, 0, -1\}$ .]

Table 4: [Ordering of eigenvalues (non-monotone non-symmetric symbol,  $f(\theta) = -e^{i\theta} + 1 + e^{-i\theta} + e^{-2i\theta} + e^{-3i\theta}$ )  $\hat{T}_n(f) = T_{n,\varepsilon,\varphi}(f)$  for all combinations  $\varepsilon, \varphi = \{-1, 0, -1\}$ . Coloring indicate erroneous ordering, with same color as corresponding panel in Figure 11.]

| $\lambda_j(H_n(f))$ | (-1, -1)       | (-1, 0)        | (-1, 1)        | (0, -1)        | (0, 0)         | (0, 1)         | (1, -1)        | (1, 0)         | (1, 1)         |
|---------------------|----------------|----------------|----------------|----------------|----------------|----------------|----------------|----------------|----------------|
| -3.0752             | <b>3.0752</b>  | <b>3.0752</b>  | 2.6384         | <b>3.0752</b>  | <b>3.0752</b>  | 2.6384         | 2.6384         | 2.6384         | 2.6384         |
| -1.9512             | <b>-3.1066</b> | -3.0752        |
| -1.8592             | 2.6384         | 2.6384         | <b>3.0752</b>  | 2.6384         | 2.6384         | <b>3.0752</b>  | <b>3.0752</b>  | <b>3.0752</b>  | 3.1066         |
| -1.2696             | -1.9512        | -1.9512        | -1.9512        | -1.9512        | -1.9512        | -1.9512        | -1.9512        | -1.9512        | -1.9512        |
| -1.0765             | 1.2089         | <b>1.2696</b>  | <b>1.2696</b>  | <b>1.2696</b>  | 1.2089         | 1.4612         | <b>1.2696</b>  | 1.4612         | <b>1.8592</b>  |
| 1.2089              | -1.2696        | -1.0765        | -1.0765        | -1.0765        | -1.0765        | -1.0765        | -1.0765        | -1.0765        | -1.0765        |
| 1.4612              | 1.8166         | 1.4612         | 1.4612         | 1.4612         | 1.4612         | 1.2089         | 1.4612         | 1.2089         | 1.2089         |
| 1.8166              | -1.8592        | -1.8592        | -1.8592        | -1.8592        | -1.8592        | <b>-1.8166</b> | -1.8592        | <b>-1.8166</b> | <b>-1.4612</b> |
| 2.6384              | 1.4612         | 1.8166         | 1.8166         | 1.8166         | 1.8166         | <b>1.8592</b>  | 1.8166         | <b>1.8592</b>  | 1.8166         |
| 3.1066              | -1.0765        | <b>-1.2089</b> | <b>-1.2089</b> | <b>-1.2089</b> | -1.2696        | -1.2696        | <b>-1.2089</b> | -1.2696        | -1.2696        |

Table 5: [Ordering of eigenvalues (non-monotone non-symmetric symbol,  $f(\theta) = -e^{i\theta} + 1 + e^{-i\theta} + e^{-2i\theta} + e^{-3i\theta}$ )  $\hat{T}_n(f) = T_{n,\varepsilon,\varphi}(f)$  for all combinations  $\varepsilon, \varphi = \{-1, 0, -1\}$ . Reordering to correct orderings in Table 4.]

| $\lambda_j(H_n(f))$ | (-1, -1) | (-1, 0) | (-1, 1) | (0, 1)  |
|---------------------|----------|---------|---------|---------|
|                     | (0, -1)  | (1, -1) | (1, 0)  |         |
|                     | (0, 0)   |         | (1, 1)  |         |
| -3.0752             | 3.1066   | 3.1066  | 2.6384  | 2.6384  |
| -1.9512             | -3.0752  | -3.0752 | -3.0752 | -3.0752 |
| -1.8592             | 2.6384   | 2.6384  | 3.1066  | 3.1066  |
| -1.2696             | -1.9512  | -1.9512 | -1.9512 | -1.9512 |
| -1.0765             | 1.2089   | 1.2089  | 1.2089  | 1.4612  |
| 1.2089              | -1.2696  | -1.0765 | -1.0765 | -1.0765 |
| 1.4612              | 1.8166   | 1.4612  | 1.4612  | 1.2089  |
| 1.8166              | -1.8592  | -1.8592 | -1.8592 | -1.8592 |
| 2.6384              | 1.4612   | 1.8166  | 1.8166  | 1.8166  |
| 3.1066              | -1.0765  | -1.2696 | -1.2696 | -1.2696 |

A probable reason for the failure of Algorithm 1 in this example, is that  $R_n$  has too many non-zero entries. A possible remedy could be to split up  $R_n$  to multiple matrices  $R_n^{(i)}$ , and have multiple  $\gamma_k^{(i)}$ , such that,

$$T_n(g) = \hat{T}_n(g) + \gamma_k^{(1)} R_n^{(1)} + \gamma_k^{(2)} R_n^{(2)} + \dots + \gamma_k^{(s)} R_n^{(s)}, \quad (29)$$

and first let all  $\gamma_k^{(i)}$  be zero, increase  $\gamma_k^{(1)}$  to one, then  $\gamma_k^{(2)}$ , and so on. Another approach to find the true ordering in a case like this to generate a sequence of grids, and then use a matrix-less method, and if the result is non-erratic it can be assumed to be the correct grid.

## Eigenvectors

Under the assumption that the Fourier coefficients are real, the eigenvectors of  $H_n(f)$  are the same as the corresponding either left or right singular vectors of  $T_n(f)$  (and eigenvectors either of  $(T_n(f))^T T_n(f)$  or of  $T_n(f)(T_n(f))^T$ ).

**Proof 6** Using the singular value decomposition we know that  $T_n(f) = U\Sigma V$ , where  $U, V$  are unitary and  $\Sigma$  is diagonal with the singular values ordered non-increasingly. Now  $H_n(f) = Y_n T_n(f)$  is real symmetric and hence it admits the Schur decomposition in the form  $QDQ^T$  where  $Q$  is real orthogonal. However,  $Y_n T_n(f) = Y_n U \Sigma V$  is automatically a singular value decomposition of  $Y_n T_n(f)$ , since  $Y_n$  is unitary and hence  $Y_n U = W$  is the unitary matrix containing the left singular vectors of  $Y_n T_n(f)$ . In addition, since  $Y_n T_n(f)$  is real symmetric its eigenvalues are real and due to its normality the singular values are the moduli of the eigenvalues. In other terms we have

$$D_{j,j} = \Sigma_{j,j} (-1)^{\alpha_j}, \quad \alpha_j \in \{0, 1\},$$

that is  $D = \Sigma S$  with  $S$  phase matrix such that  $D_{j,j} = (-1)^{\alpha_j}$ . From this we deduce

$$H_n(f) = QDQ^T = QS\Sigma Q^T = Q\Sigma SQ^T$$

where the latter two, up to reordering, represent the singular value decomposition of  $H_n(f)$  and the proof is over.

Now, for analyzing the signs  $(-1)^{\alpha_j}$  are distributed, it is enough to recall that the sequence  $\{T_n(f)\}$  is distributed in the singular value sense as  $f$  while,  $\{H_n(f)\}$  is distributed as  $\pm|f|$  (see [16, 11, 12, 19, 18]): from this we deduce that

$$\lim_{n \rightarrow \infty} \sum_{j=1}^n \frac{(-1)^{\alpha_j}}{n} = 0$$

and therefore, up to  $o(n)$  outliers, there is around  $n/2$  positive signs and  $n/2$  negative signs. In the case where the minimum of  $|f|$  is zero, we do not have outliers. Furthermore in the case where  $f$  is smooth, up to a negligible number of outliers the eigenvalues of  $H_n(f)$  can be seen as a sampling of  $\pm|f|$ : the number of these outliers all with modulus less than  $\min|f|$  can be bounded by a constant independent of  $n$ , when  $f$  is also a trigonometric polynomial.

## 4 Conclusions

In a series of recent papers the spectral behavior of the matrix sequence  $\{Y_n T_n(f)\}$  has been studied in the sense of the spectral distribution, with  $f$ , the generating function, being Lebesgue integrable and with real Fourier coefficients. This kind of study is also motivated by computational purposes for the solution of the related large linear systems using the (preconditioned) MINRES algorithm. Here we have complement the spectral study with more results holding both asymptotically and for a fixed dimension  $n$ : the final target is the design of ad hoc procedures for the computation of the related spectra via matrix-less algorithms, with a cost being linear in the number of computed eigenvalues. We emphasize that in this note we have treated the challenge of the case of non-monotone generating functions, for which the previous matrix-less algorithms fail. Numerical experiments have been reported and commented, with the aim of showing in a visual way the theoretical analysis.

## References

- [1] D. BINI AND M. CAPOVANI, *Spectral and computational properties of band symmetric Toeplitz matrices*, Linear Algebra and its Applications, 52-53 (1983), pp. 99–126.
- [2] E. BOZZO AND C. D. FIORE, *On the use of certain matrix algebras associated with discrete trigonometric transforms in matrix displacement decomposition*, SIAM Journal on Matrix Analysis and Applications, 16 (1995), pp. 312–326.
- [3] A. BÖTTCHER AND S. M. GRUDSKY, *On the condition numbers of large semidefinite Toeplitz matrices*, Linear Algebra and its Applications, 279 (1998), pp. 285–301.
- [4] A. BÖTTCHER AND B. SILBERMANN, *Introduction to Large Truncated Toeplitz Matrices*, Springer New York, 1999.
- [5] A. CANTONI AND P. BUTLER, *Eigenvalues and eigenvectors of symmetric centrosymmetric matrices*, Linear Algebra and its Applications, 13 (1976), pp. 275–288.
- [6] P. DELSARTE AND Y. GENIN, *Spectral properties of finite Toeplitz matrices*, in Mathematical Theory of Networks and Systems, Springer-Verlag, pp. 194–213.
- [7] S.-E. EKSTRÖM, I. FURCI, AND S. SERRA-CAPIZZANO, *Exact formulae and matrix-less eigensolvers for block banded symmetric Toeplitz matrices*, BIT Numerical Mathematics, 58 (2018), pp. 937–968.
- [8] S.-E. EKSTRÖM AND C. GARONI, *A matrix-less and parallel interpolation-extrapolation algorithm for computing the eigenvalues of preconditioned banded symmetric toeplitz matrices*, Numerical Algorithms, 80 (2019), p. 819–848.
- [9] S.-E. EKSTRÖM, C. GARONI, A. JOZEFIAK, AND J. PERLA, *Eigenvalues and eigenvectors of tau matrices with applications to Markov processes and economics*, Linear Algebra and its Applications, 627 (2021), pp. 41–71.
- [10] S.-E. EKSTRÖM, C. GARONI, AND S. SERRA-CAPIZZANO, *Are the eigenvalues of banded symmetric Toeplitz matrices known in almost closed form?*, Experimental Mathematics, 27 (2018), pp. 478–487.
- [11] P. FERRARI, I. FURCI, S. HON, M. A. MURSALEEN, AND S. SERRA-CAPIZZANO, *The eigenvalue distribution of special 2-by-2 block matrix-sequences with applications to the case of symmetrized Toeplitz structures*, SIAM Journal on Matrix Analysis and Applications, 40 (2019), pp. 1066–1086.
- [12] P. FERRARI, I. FURCI, AND S. SERRA-CAPIZZANO, *Multilevel symmetrized Toeplitz structures and spectral distribution results for the related matrix sequences*, Electronic Journal of Linear Algebra, 37 (2021), pp. 370–386.
- [13] C. GARONI AND S. SERRA-CAPIZZANO, *Generalized locally Toeplitz sequences: theory and applications. Vol. I*, Springer International Publishing, Cham, 2017.
- [14] ———, *Generalized locally Toeplitz sequences: theory and applications. Vol. II*, Springer International Publishing, 2018.
- [15] U. GRENANDER AND G. SZEGŐ, *Toeplitz Forms and Their Applications*, Chelsea, New York, 1984. Second edition.
- [16] S. HON, M. A. MURSALEEN, AND S. SERRA-CAPIZZANO, *A note on the spectral distribution of symmetrized Toeplitz sequences*, Linear Algebra and its Applications, 579 (2019), pp. 32–50.

- [17] M. MAZZA AND J. PESTANA, *Spectral properties of flipped Toeplitz matrices and related preconditioning*, BIT Numerical Mathematics, 59 (2018), pp. 463–482.
- [18] M. MAZZA AND J. PESTANA, *The asymptotic spectrum of flipped multilevel Toeplitz matrices and of certain preconditionings*, SIAM Journal on Matrix Analysis and Applications, 42 (2021), pp. 1319–1336.
- [19] J. PESTANA, *Preconditioners for symmetrized Toeplitz and multilevel Toeplitz matrices*, SIAM Journal on Matrix Analysis and Applications, 40 (2019), pp. 870–887.
- [20] S. SERRA-CAPIZZANO, *On the extreme eigenvalues of hermitian (block) Toeplitz matrices*, Linear Algebra and its Applications, 270 (1998), pp. 109–129.
- [21] ———, *Spectral behavior of matrix sequences and discretized boundary value problems*, Linear Algebra and its Applications, 337 (2001), pp. 37–78.
- [22] S. SERRA-CAPIZZANO, D. BERTACCINI, AND G. H. GOLUB, *How to deduce a proper eigenvalue cluster from a proper singular value cluster in the nonnormal case*, SIAM Journal on Matrix Analysis and Applications, 27 (2005), pp. 82–86.
- [23] S. SERRA-CAPIZZANO AND C. TABLINO POSSIO, *Analysis of preconditioning strategies for collocation linear systems*, Linear Algebra and its Applications, 369 (2003), pp. 41–75.
- [24] P. TILLI, *A note on the spectral distribution of toeplitz matrices*, Linear and Multilinear Algebra, 45 (1998), pp. 147–159.
- [25] ———, *Some results on complex Toeplitz eigenvalues*, Journal of Mathematical Analysis and Applications, 239 (1999), pp. 390–401.
- [26] L. N. TREFETHEN, *Pseudospectra of matrices*, Numerical analysis, 91 (1991), pp. 234–266.
- [27] E. TYRTYSHNIKOV AND N. ZAMARASHKIN, *Spectra of multilevel toeplitz matrices: Advanced theory via simple matrix relationships*, Linear Algebra and its Applications, 270 (1998), pp. 15–27.
- [28] E. E. TYRTYSHNIKOV, *A unifying approach to some old and new theorems on distribution and clustering*, Linear Algebra and its Applications, 232 (1996), pp. 1–43.